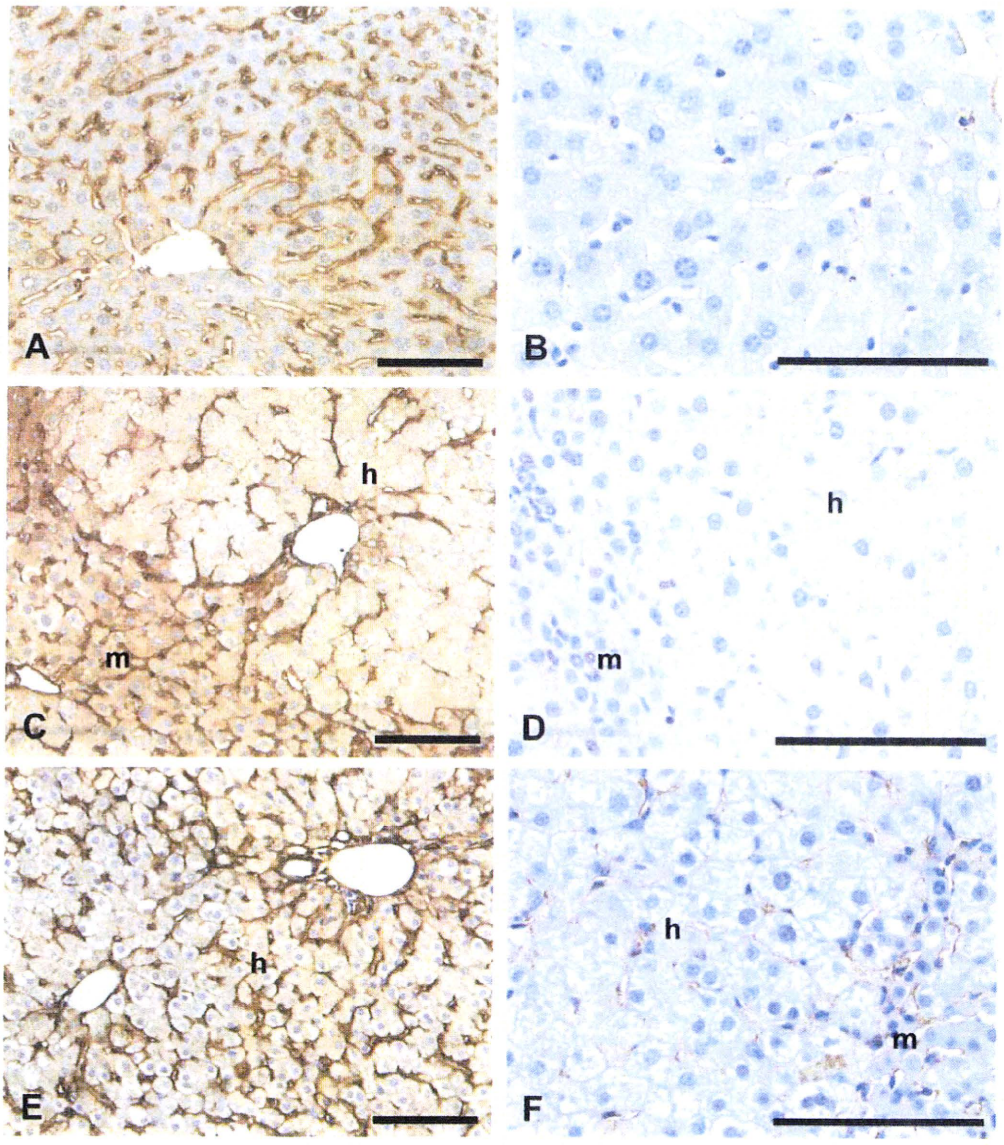

FIGURE 4.—Hepatic cord reconstruction and sinusoid endothelial cell lining in the urokinase-type plasminogen activator transgenic/severe combined immunodeficiency (uPA$^{+/+}$/SCID) chimeric mouse liver. uPA$^{WT/WT}$/SCID mouse (A and B) and uPA$^{+/+}$/SCID chimeric mouse with lower RI (C and D: RI = 68%) and higher RI (E and F: RI = 95%) livers were shown. Laminin immunohistochemistry (A, C, and E) revealed immature (C) and differentiating (E) hepatic cords lined by the basement membrane in human hepatocyte area (h) compared with uPA$^{WT/WT}$/SCID mouse liver (A). In the donor mouse hepatocyte area (m) laminin-positive filaments appear to surround degenerating mouse hepatocytes (C). CD31-positive sinusoid endothelial cells accompanied laminin-positive basement membrane in the livers (B, D, and F) and there were few CD31-positive cells in the proliferating human hepatocyte nodule (D). WT, wild type; RI, replacement index; Bar = 100 μm.

1991). Meuleman et al. (2005) morphologically and biochemically characterized chimeric livers from uPA$^{+/+}$/SCID mice repopulated with human hepatocytes and successfully infected them with HBV and HCV. Similar to our study, the transplanted human hepatocytes were swollen with clear cytoplasm, and the plasma of the chimeric mice contained hAlb as well as 21 additional human proteins (Meuleman et al., 2005). Prior mRNA-expression analysis of our uPA$^{+/+}$/SCID chimeric livers demonstrated expression of 20 human CYPs, 26 human phase II metabolic enzymes, and 21 human transporters (Nishimura et al., 2005). The reported mRNA expression profiles of CYP2E1, CYP3A4, and CYP3A5 mRNAs are consistent with protein localization of these CYPs to the human hepatocyte areas in our IHC study. Other animal models with humanized livers, including immunodeficient (Pfp/Rag2) mice (Aurich et al., 2007) and rats (Ho et al., 2005; Ouyang et al., 2001), have shown that it may be possible to transplant human hepatocytes into the livers; however, extensive morphologic, immunohistochemical,

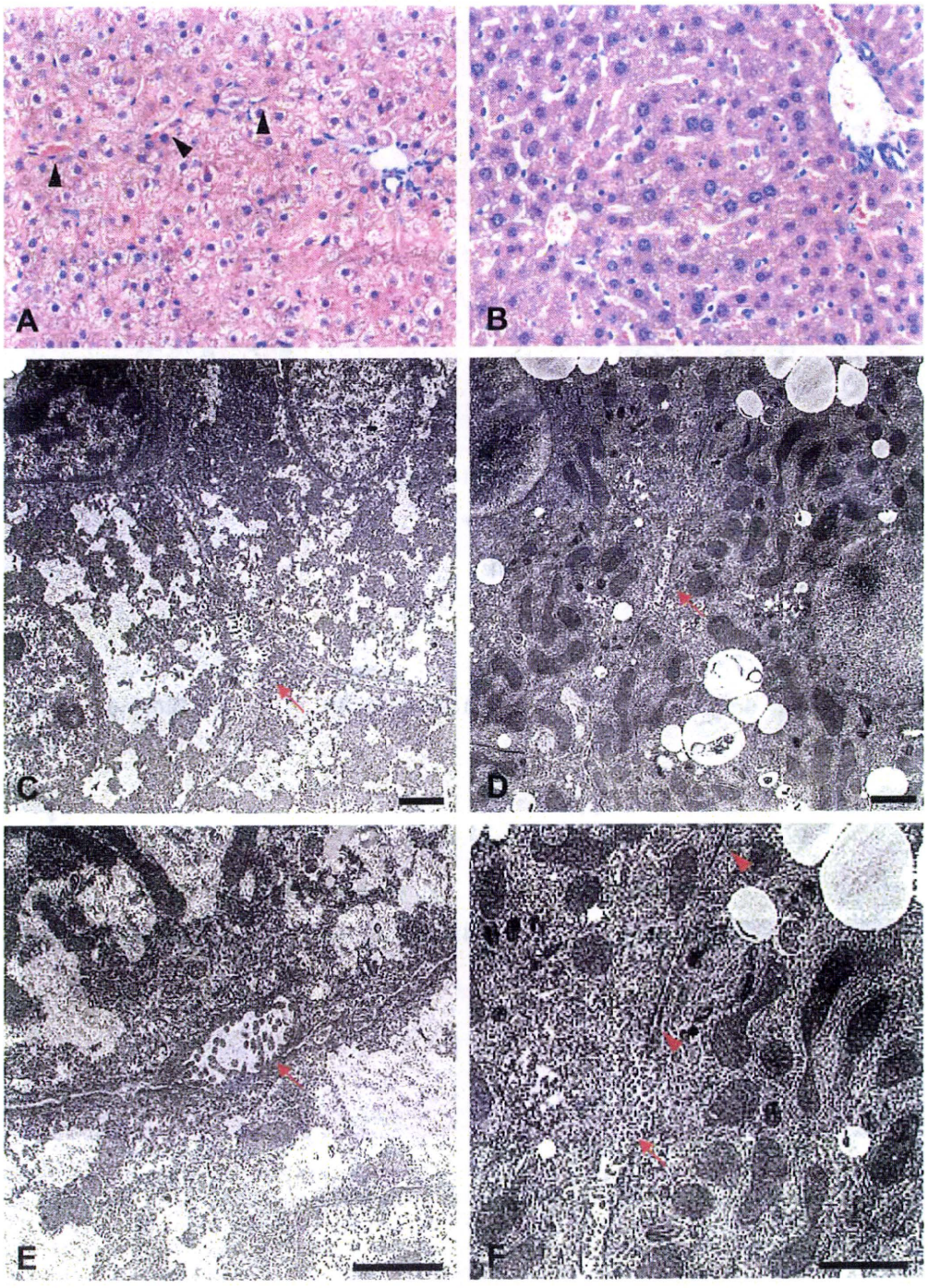

FIGURE 5.—Histomorphological and ultrastructural analyses of the liver of urokinase-type plasminogen activator transgenic/severe combined immunodeficiency (uPA$^{+/+}$/SCID) chimeric mice (A, C, and E) and uPA$^{WT/WT}$/SCID mice (B, D, and F). In well-differentiated human hepatocyte areas (RI = 95%) human hepatocytes exhibited trabeculae and hepatic-cord patterns (A). Sinusoid-like structure (black arrowheads) lined by endothelial cells were observed, but Kupffer cells were not apparent in the human hepatocyte area (A). Electron microscopy observations revealed bile canaliculi (red arrows) among hepatocytes in both uPA$^{+/+}$/SCID chimeric mice (C and E) and uPA$^{WT/WT}$/SCID mice (D and F). Tight junctions were observed in uPA$^{WT/WT}$/SCID mice (red arrowheads) but were not apparent in uPA$^{+/+}$/SCID chimeric mice. WT, wild type; RI, replacement index. Bar = 1 μm.

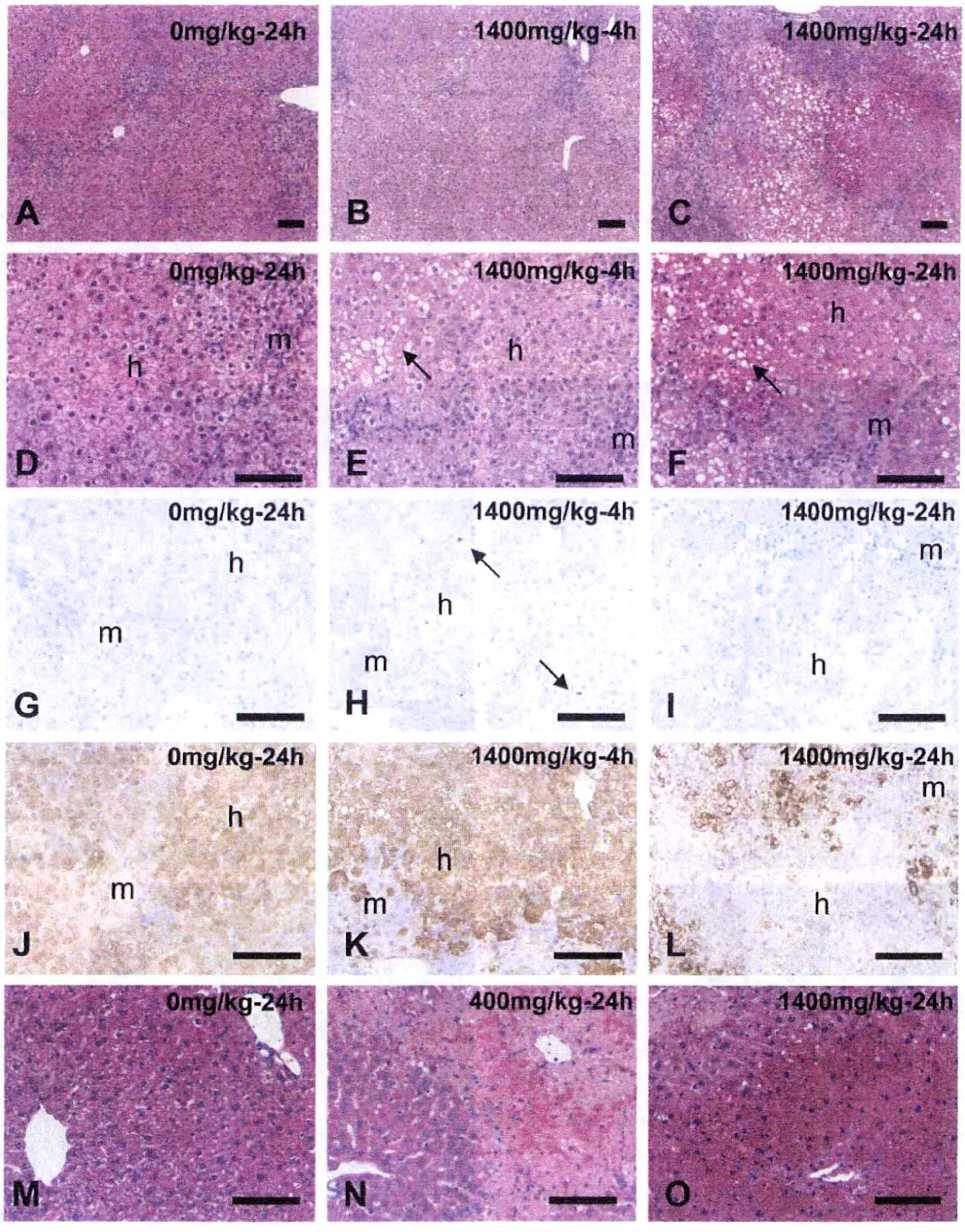

FIGURE 6.—The toxicological response of the humanized livers following acetaminophen (APAP) administration was evaluated in the chimeric mice (A–L) and compared with that of the livers of ICR mice (M–O). Lines from left: Chimeric mice 24 h after administration of 0 mg/kg APAP (A, D, G, and J), 4 h after administration of 1,400 mg/kg (B, E, H, and K), and 24 h after administration of 1,400 mg/kg (C, F, I, and L). Results revealed treatment-related hepatocellular vacuolation (E; arrow) and degeneration (F; arrow), apoptotic hepatocytes (H; arrow), and reduced expression of CYP2E1 (L) in the human hepatocyte area (h). APAP-related changes were not observed in the mouse hepatocyte area (m) of the chimeric mice. In the ICR mouse livers, administration of APAP at 400 mg/kg (N) or 1,400 mg/kg (O) resulted in massive destruction of liver tissue and zonal hemorrhage 24 h postdose. All ICR mice that received 1,400 mg/kg of APAP died within 24 h postdose (O). A–F and M–O, hematoxylin and eosin staining; G–I, TUNEL method; J–L, CYP2E1 immunohistochemistry corresponding to G–I, respectively. TUNEL, TdT-dUTP nick end labeling. Bar = 100 μm.

and ultrastructural characterization of the humanized livers has not been previously described.

In the present study, we demonstrate that transplanted human hepatocytes express human CYPs, MRPs, and PGP in the murine liver following repopulation; in addition, the toxicologic response to APAP in these chimeric mice is less dramatic than that in nonchimeric (ICR) mice.

High doses of APAP produce centrilobular hepatic necrosis, mediated by CYP-dependent metabolism (CYP2E1, CYP3A4, and CYP1A2) to N-acetyl-p-benzoquinone imine (NAPQI; Dahlin

et al., 1984). APAP-induced hepatic injury is increased by depletion of glutathione and formation of covalent adducts with hepatic proteins, and these subsequent changes are mediated by NAPQI. Furthermore, NAPQI induces oxidant stress (peroxynitrate) and mitochondria-mediated cell death (Latchoumycandane et al., 2007). In addition, an in vitro examination using human hepatoma cells (Bel-7402) revealed that the cytotoxic effects of APAP were increased in the presence of S9 mixture (Zhang et al., 2007). These results indicate that APAP is a metabolism-mediated cytotoxicant for both rodents and humans.

Some transgenic mouse studies indicate that metabolism-related factors and transporter expression are necessary for the hepatotoxic effects of APAP. CYP2E1 knockout (KO; El-Hassan et al., 2003; Lee et al., 1996), Mrp3 KO (Manautou et al., 2005), CAR (constitutive androstane receptor, a key regulator of APAP metabolism) KO (Zhang et al., 2002), and SOD1 (Cu,Zn-superoxide dismutase) KO (Lei et al., 2006) mice have been shown to be more resistant to APAP toxicity. In the SOD1 KO mice, a reduction in CYP2E1 activity (as opposed to CYP2E1 protein) attenuates APAP toxicity. Although all these KO mice seem to have normal phenotypes, survival rates and tolerance to APAP are generally higher than those of the corresponding wild-type mice. The toxic effects in the wild-type mice with 400–600 mg/kg APAP were similar to those in ICR mice in our study. By comparison, our uPA$^{+/+}$/SCID chimera livers contained more differentiated hepatocytes than in vitro human hepatoma cells, and the hepatocytes in these chimeric liver expressed human CYP, MRP, and PGP proteins. Although CYP and MRP activities were not measured, the immunoexpression level of CYP2E1 was reduced in the human hepatocyte area 24 h after APAP administration. Our findings that uPA$^{+/+}$/SCID chimeric mice better tolerated APAP toxicity might suggest that the metabolizing proteins were not fully activated in the liver. Furthermore, immature hepatocytes such as oval cells are reported to be resistant to APAP injury (Kofman et al., 2005). Thus, the reduced toxicity to APAP in uPA$^{+/+}$/SCID chimeric mice may be due to functional immaturity of the repopulating human hepatocytes. Quantification of NAPQI and exposure level of APAP in treated ICR mouse liver, mouse and human hepatocyte areas of chimeric mouse liver, and uPA$^{WT/WT}$/SCID mouse liver might identify the cause of the differences in APAP toxicity among these mice. There may also be other factors contributing to this difference. Michael et al. (1999) showed the importance of hepatic macrophages in APAP toxicity. In addition, Liu et al. (2006) used intracellular adhesion molecule-1-deficient mice to demonstrate that neutrophil accumulation contributes to the progression of APAP-induced hepatotoxicity. In the present study, histopathological examination of the uPA$^{+/+}$/SCID chimeric mice showed that nonparenchymal cells (such as Kupffer cells and sinusoid endothelial cells) were not clearly observed in the areas of proliferating human hepatocytes and that there were no inflammatory reactions in the liver associated with APAP administration. The absence of inflammatory cell or Kupffer cell activity might also attenuate the APAP hepatotoxicity in the uPA$^{+/+}$/SCID chimeric mice. Vacuolation and degeneration of human hepatocytes were induced by APAP, but severe necrosis was not observed in the chimeric mouse livers. The influence of nafamostat administration and the genetic background of the SCID mouse on the inflammatory cell reactions will be addressed in subsequent investigations.

Thus, the mechanisms by which APAP exerts its toxic effects are incompletely understood, even in rodents. At present, there is no evidence of species differences in the mechanisms underlying APAP toxicity or APAP sensitivity. The present study revealed clear differences in APAP toxicity levels between the uPA$^{+/+}$/SCID chimeric and ICR mice, but the results were obtained in partially humanized livers (RI < 95%), not a "completely" humanized liver. We believe this animal model will continue to be a useful tool to investigate drug metabolism, hepatotoxicity, and idiosyncratic liver diseases of humans.

In conclusion, human hepatocyte-transplanted chimeric mice contain viable, differentiating, and proliferating human hepatocytes in the liver. The transplanted human hepatocytes express human proteins, develop complex architectural features (bile canaliculi and hepatic cords), providing an "in vivo" murine approach to investigate human liver function.

ACKNOWLEDGMENTS

We acknowledge Mamoru Takahashi (Pfizer Global R&D) for technical assistance in electron microscopy examinations and Dr. Anne M. Ryan (Pfizer Global R&D) for scientific review of the manuscript.

REFERENCES

Aurich, I., Mueller, L. P., Aurich, H., Luetzkendorf, J., Tisljar, K., Dollinger, M. M., Schormann, W., Walldorf, J., Hengstler, J. G., Fleig, W. E., and Christ, B. (2007). Functional integration of hepatocytes derived from human mesenchymal stem cells into mouse livers. *Gut* **56,** 405–415.

Dahlin, D. C., Miwa, G. T., Lu, A. Y. N., and Nelson, S. D. (1984). N-Acetyl-p-benzoquinone imine: a cytochrome P-450-mediated oxidation product of acetaminophen. *Proc Natl Acad Sci U S A* **81,** 1327–1331.

Dandri, M., Burda, M., Török, E., Pollok, J. M., Iwanska, A., Sommer, G., Rogiers, X., Rogler, C. E., Gupta, S., Will, H., Greten, H., and Peterson, J. (2001). Repopulation of mouse liver with human hepatocytes and in vivo infection with hepatitis B virus. *Hepatology* **33,** 981–988.

El-Hassan, H., Anwar, K., Macanas-Pirard, P., Crabtree, M., Chow, S. C., Johnson, V. L., Lee P. C., Hinton, R. H., Price, S. C., and Kass, E. N. (2003). Involvement of mitochondria in acetaminophen-induced apoptosis and hepatic injury: roles of cytochrome C, Bax, Bid, and caspases. *Toxicol Appl Pharmol* **191,** 118–129.

Ho, W. J., Ho, C. D., Hoon, K. J., Ja, K. S., Jeong, C. H., Su, L. N., and Sook, P. H. (2005). Human mesenchymal stem cells injected via portal vein are differentiated into human hepatocytes in regenerating rat liver. *Blood* **106,** 483A.

Katoh, M., and Yokoi, T. (2007) Application of chimeric mice with humanized liver for predictive ADME. *Drug Metab Rev* **39,** 145–157.

Kofman, A. V., Morgan, G., Kirschenbaum, A., Osbeck, J., Hussen, M., Swenson, S., and Theise, N. D. (2005). Dose- and time-dependent oval cell reaction in acetaminophen-induced murine liver injury. *Hepatology* **41,** 1252–1261.

Latchoumycandane, C., Goh, C. W., Ong, M. M. K., and Boelsterli, U. A. (2007). Mitochondrial protection by the JNK inhibitor leflunomide rescues mice from acetaminophen-induced liver injury. *Hepatology* **45,** 412–421.

Lee, S. S. T., Buters, J. T., Pineau, T., Fernandez-Salguero, P., and Gonzalez, F. J. (1996). Role of CYP2E1 in the hepatotoxicity of acetaminophen. *J Biol Chem* **20,** 12063–12067.

Lei, X. G., Zhu, J. H., McClung, J. P., Aregullin, M., and Roneker, C. A. (2006) Mice deficient in Cu,Zn-superoxide dismutase are resistant to acetaminophen toxicity. *Biochem J* **399,** 455–461.

Liu, Z. X., Han, D., Gunawan, B., and Kaplowitz, N. (2006) Neutrophil depletion protects against murine acetaminophen hepatotoxicity. *Hepatology* **43,** 1220–1230.

Manautou, J. E., de Waart, D. R., Kunne, C., Zelcer, N., Goedken, M., Borst, P., and Elferink, R. O. (2005). Altered disposition of acetaminophen in mice with a disruption of the *Mrp3* gene. *Hepatology* **42,** 1091–1098.

Mercer, D. F., Schiller, D. E., Elliott, J. F., Douglas, D. N., Hao, C., Rinfret, A., Addison, W. R., Fischer, K. P., Churchill, T. A., Lakey, J. R., Tyrrell, D. L., and Kneteman, N. M. (2001). Hepatitis C virus replication in mice chimeric human livers. *Nat Med* **7,** 927–933.

Meuleman, P., Libbrecht, L., De Vos, R., de Hemptinne, B., Gevaert, K., Vandekerckhove, J., Roskams, T., and Leroux-Roels, G. (2005). Morphological and biochemical characterization of a human liver in a uPA-SCID mouse chimera. *Hepatology* **41,** 847–856.

Michael, S. L., Pumford, N. R., Mayeux, P. R., Niesman, M. R., and Hinson, J. A. (1999). Pretreatment of mice with macrophage inactivators decreases acetaminophen hepatotoxicity and the formation of reactive oxygen and nitrogen species. *Hepatology* **30,** 186–195.

Nishimura, M., Yoshitsugu, H., Yokoi, T., Tateno, C., Kataoka, N., Horie, T., Yoshizato, K., and Naito, S. (2005). Evaluation of mRNA expression of human drug-metabolizing enzymes and transporters in chimeric mouse with humanized liver. *Xenobiotica* **35,** 877–890.

Ouyang, E. C., Wu, C. H., Walton, C., Promrat, K., and Wu, G. Y. (2001). Transplantation of human hepatocytes into tolerized genetically immunocompetent rats. *World J Gastroenterol* **7,** 324–330.

Sandgren, E. P., Palmiter, R. D., Heckel, J. L., Daugherty, C. C., Brinster, R. L., and Degen, J. L. (1991). Complete hepatic regeneration after somatic deletion of an albumin-plasminogen activator transgenic. *Cell* **66,** 245–256.

Tateno, C., Yoshizane, Y., Saito, N., Kataoka, M., Utoh, R., Yamasaki, C., Tachibana, A., Soeno, Y., Asahina, K., Hino, H., Asahara, T., Yokoi, T., Furukawa, T., and Yoshizato, K. (2004). Near completely humanized liver in mice shows human-type metabolic responses to drugs. *Am J Pathol* **165,** 901–912.

Tsuge, M., Hiraga, N., Takaishi, H., Noguchi, C., Oga, H., Imamura, M., Takahashi, S., Iwao, E., Fujimoto, Y., Ochi, H., Chayama, K., Tateno, C., and Yoshizato, K. (2005). Infection of human hepatocyte chimeric mice with genetically engineered hepatitis B virus. *Hepatology* **42,** 1046–1054.

Zhang, J., Huang, W., Chua, S. S., Wei, P., and Moore, D. D. (2002). Modulation of acetaminophen-induced hepatotoxicity by the xenobiotic receptor CAR. *Science* **298,** 422–424.

Zhang, L., Mu, X., Fu, J., and Zhou, Z. (2007) In vitro cytotoxicity assay with selected chemicals using human cells to predict target-organ toxicity of liver and kidney. *Toxicol in Vitro* **21,** 734–740.

MOLECULAR CARCINOGENESIS 47:784–796 (2008)

Pleiotrophin Inhibits Transforming Growth Factor β1-Induced Apoptosis in Hepatoma Cell Lines

Tae Jun Park,[1] Bo Ra Jeong,[1] Chise Tateno,[2] Hong Seok Kim,[1] Tomohiro Ogawa,[3,4] In Kyoung Lim,[1] and Katsutoshi Yoshizato[2,3,4]*

[1]*Biochemistry and Molecular biology, School of Medicine, Ajou University, Suwon, South Korea*
[2]*Yoshizato Project, Cooperative Link of Unique Science and Technology for Economy Revitalization (CLUSTER), Hiroshima Prefectural Institute of Industrial Science and Technology, Higashihiroshima, Japan*
[3]*Developmental Biology Laboratory, Department of Biological Science, Graduate School of Science, Higashihiroshima, Japan*
[4]*Hiroshima University 21st Century COE Program for Advanced Radiation Casualty Medicine, Hiroshima Liver Project Research Center, Hiroshima University, Hiroshima, Japan*

Pleiotrophin (PTN) is a hepatocyte growth factor and considered to play roles in liver fibrogenesis and hepatocarcinogenesis. In this study we examined the mechanism of the action of PTN in these pathological processes. First, we confirmed that hepatic stellate cells (HSCs) and Kupffer cells, and also later hepatocytes in hyperplastic nodules increased PTN mRNA expressions during carbon tetrachloride-induced liver fibrosis. Then, the relationship between PTN and transforming growth factor β1 (TGFβ1), a known potent pro-fibrogenetic cytokine, in carcinogenesis was investigated using hepatoma cell lines. Huh-7 human hepatoma cells weakly expressed PTN, but HepG2 human hepatoma cells and FaO rat hepatoma cells did not. Recombinant (r) TGFβ1 induced the cultured Huh-7 cells to undergo apoptosis, which was inhibited by rPTN. Huh-7 cells became resistant to TGFβ1-, but not mitomycin C-induced apoptosis when transfected with PTN gene, indicating the specificity of the PTN anti-apoptotic activity. Poly ADP ribose polymerase, procaspase-8 and procaspase-3 were not cleaved in the TGFβ1-reluctant cells. The TGFβ1-induced caspase-3 activation was also suppressed in Huh-7 and FaO cells both transduced with PTN gene-bearing adenoviruses. In summary, PTN was expressed in HSCs, Kupffer cells, and hepatocytes in fibrotic liver. We propose that PTN specifically antagonizes the TGFβ1 activity during liver fibrosis.

Key words: pleiotrophin; TGFβ1; liver fibrosis; hepatocarcinogenesis; caspase-3; hepatic stellate cells

INTRODUCTION

Pleiotrophin (PTN) is a multifunctional cytokine involved in growth, transformation, carcinogenesis, and metastasis [1]. PTN is an 18 kDa heparin binding protein and shows 50% identity to midkine (MK) [2–4]. It promotes the growth of fibroblasts, endothelial cells, and hepatocytes [4–6]. Its gene is grouped as a potent proto-oncogene [7–8]. PTN transforms NIH 3T3 cells in a soft agar plate, and forms highly vascularized tumors [1]. Up-regulation of PTN gene promotes tumor angiogenesis [7]. Furthermore, PTN acts as an angiogenic factor in a paracrine mode for human breast cancer, choriocarcinoma, and melanoma, and seems to be essential for the development of metastasis in melanoma [8].

Previously we identified PTN as a mitogen for rat hepatocytes [9] among proteins secreted by Swiss 3T3 fibroblasts, indicating that PTN plays a role as a hepatocyte growth factor. When co-cultured, rat hepatic stellate cells (HSCs) enhanced the growth of rat hepatocytes by secreting PTN [6]. Furthermore, PTN expression was increased in carbon tetrachloride (CCl_4)-induced fibrotic liver [10]. However, the biological mechanism of PTN in hepatocarcinogenesis has not been clarified yet.

Liver cirrhosis and hepatocellular carcinoma are among the most common liver diseases, and several mechanisms involved in carcinogenesis have been proposed [11–13]. Transforming growth factor β1 (TGFβ1) has been known as a potent fibrogenesis factor [14]. TGFβ1 shows multiple biological properties, including the inhibition of proliferation, the induction of apoptosis, the activation of HSCs, and the promotion of extracellular matrix formation. TGFβ1 expression is low in normal liver, elevated in livers of patients with acute hepatitis, fulminant

Abbreviations: PTN, pleiotrophin; HSC, hepatic stellate cell; CCl_4, carbon tetrachloride; TGFβ1, transforming growth factor β1; PARP, ADP ribose polymerase; PTN-Ad, pleiotrophin adenovirus; LacZ-Ad, LacZ adenovirus.

Chise Tateno's and Katsutoshi Yoshizato's present address is PhoenixBio Co. Ltd., 3-4-1 Kagamiyama, Higashihiroshima, Japan.

*Correspondence to: PhoenixBio. Co. Ltd., 3-4-1 Kagamiyama, Higashihiroshima, Hiroshima 739-0046, Japan.

Received 30 November 2007; Revised 4 February 2008; Accepted 11 February 2008

DOI 10.1002/mc.20438

Published online 31 March 2008 in Wiley InterScience (www.interscience.wiley.com)

hepatic failure, and liver cirrhosis [15]. TGFβ1 is a potent inhibitor of DNA synthesis of cultured hepatocytes and inhibits hepatocyte proliferation after partial hepatectomy [16–18]. The inhibition of TGFβ1 signal effectively prevents fibrosis and preserves the liver function in a fibrotic animal model [19]. These studies all support that TGFβ1 plays pivotal roles in liver fibrogenesis and carcinogenesis.

Apoptosis is essential for normal development and tissue homeostasis. The deregulation of apoptosis and the accelerated proliferate activity of hepatocytes have been reported as significant steps for hepatocarcinogenesis [20,21]. During hepatocarcinogenesis, some of the genetically altered hepatocytes progress to apoptosis and some escape from the apoptosis and undergo carcinogenesis [21]. TGFβ1 is the most effective apoptotic cytokine during hepatocarcinogenesis [22]. TGFβ1 generated the reactive oxygen species and induced apoptosis of Huh-7 cells and activates first caspase-8, -9, and finally -3 [23,24]. Furthermore, a study on "the loss of TGFβ receptor" showed that the hepatocytes in diethylnitrosamine and nodularin-induced-hyperplastic liver nodules escaped from the TGFβ1-induced apoptosis and continued to proliferate [21].

In the present study, we investigated the role of PTN in TGFβ1-induced liver fibrogenesis and carcinogenesis, placing an emphasis TGFβ1-induced apoptosis of hepatocytes. We first demonstrated that HSCs expressed PTN at higher levels. The hepatocytes in hyperplastic nodules formed in a late phase of fibrogenesis started its expression. Then, we focused on the relationship of PTN and TGFβ1 in carcinogenesis using hepatoma cell lines as experimental models. Recombinant (r) PTN suppressed the rTGFβ1-induced apoptosis of cultured hepatoma cells. The mechanism of the anti-apoptotic activity of PTN was studied utilizing hepatoma cells that had been enforced to express PTN gene. The obtained results enabled us to propose that PTN suppresses the apoptosis induced by TGFβ1, but not by mitomycin C, through inhibiting the activation of procaspase-8 and procaspase-3.

MATERIALS AND METHODS

Animal

Nine weeks old Fischer 344 (F344) male rats, weighing 170–180 g, were purchased from Laboratory Animal Center (Shizuoka, Japan), and maintained with standard chow diet and water, ad libitum, under the Institution's guidelines. To induce liver fibrosis, rats were injected subcutaneously with CCl_4 (Wako Pure Chemicals, Osaka, Japan) twice a week for 10 wk at a dose of 2.0 ml/kg body weight. Control rats were injected mineral oil subcutaneously. Five animals were killed at 5, 8, and 10 wk after the CCl_4-administration.

Isolation of Hepatocytes and HSCs

Primary rat hepatocytes were isolated from livers of normal F344 male rats as described previously [25]. Briefly, livers were perfused with collagenase and hepatocytes were harvested by centrifugation at 50*g* for 5 min, and further density gradient centrifugation with 50% Percoll (Amersham, Uppsala, Sweden) at 50*g* for 24 min. The pellet was washed three times with Dulbecco's modified Eagle's medium (DMEM, Gibco BRL, Bethesda, MD), and the cell viability was measured by trypan blue dye exclusion. An HSC-enriched fraction was prepared as reported previously [26]. Briefly, rat livers were digested in situ by perfusion first with 0.07% pronase E (Merck, Darmstadt, Germany) and then with 0.03% collagenase (Wako). They were then excised, broken into small pieces, and digested with 0.08% pronase E, 0.08% collagenase, and 20 μg/ml DNase I (Roche, Mannheim, Germany). The liver cells obtained were suspended in 8.2% Nycodenz (Nycomed, Oslo, Norway) solution and centrifuged with 2,000*g* at 4°C for 20 min. The cells in the upper layer were collected as the HSC-enriched fraction, washed, and suspended in DMEM containing 10% fetal bovine serum (FBS). The mRNA expression level of α-smooth muscle actin (α-SMA) was determined by RT-PCR and used as a measure of the activation of HSCs.

RT-PCR

Total cellular RNAs were isolated from cells of human hepatoma lines (HepG2 and Huh-7), and cells of rat hepatoma cell line (FaO), rat hepatocytes, HSCs, and CCl_4-treated rats liver. First strand cDNA was synthesized using oligo-dT primers from 1 μg of total cellular RNA by reverse transcription reaction in 10 μl reaction volume. The used primers were as follows: human PTN, sense 5′-aaaatgcaggctcaacagtaccagcag-3′ and antisense 5′-cttttaatccagcatcttctcctgttt-3′; rat PTN, sense 5′-aaaatgtcgtcccagcaatacagcag-3′ and antisense 5′-cttttaatccagcatcttctcctgttt-3′; human glyceraldehyde-3-phosphate dehydrogenase (GAPDH): sense 5′-ggtgctgagtatgtcgtgga-3′ and antisense 5′-gccatgccagtgagcttccc-3′; rat GAPDH, sense 5′-ccatggagaaggctgggg-3′ and antisense 5′-caaagttgtcatggatggatgacc-3′; rat α-SMA: sense 5′-tgtgctggactctggagatc-3′ and antisense 5′-gatcacctgcccatcagg-3′. Amplification were carried out as follows: denaturation at 94°C for 30 s, annealing for 50 s, and extension at 72°C for 50 s. Annealing temperatures were 58°C except 56°C for human PTN. PCR products were separated on 1.5% agarose gels.

Immunohistochemistry

Seven-μm-thick sections were prepared from liver tissues using a cryostat, Leica CM 1900 (Leica Instruments GmbH, Nussloch, Germany), and used for immunohistochemistry with polyclonal antibodies against PTN (N15, Santa Cruz Biotechnology,

Inc., Santa Cruz, CA), α-SMA (Sigma–Aldrich, St. Louis, MO), and ED2, a rat macrophage antigen (Sigma–Aldrich). The sections were treated with 2% normal serum for 20 min, and then incubated overnight with the above antibodies followed by incubation with antibodies with Texas-red and FITC (Zymed, San Francisco, CA) for 60 min. Slides were washed and stained for nucleus with DAPI. The cells were viewed under a fluorescence microscope (Zeiss, Axio Imager M1, Germany).

Induction of Apoptosis by TGFβ1

Cells of human hepatoma cell line, Huh-7, are highly sensitive to TGFβ1 regarding the apoptotic induction [24]. Huh-7 cells were maintained in DMEM containing 10% FBS, and were treated with 1–10 ng/ml of rTGFβ1 (Peprotech EC LTD, London, England) alone or co-treated with 100 ng/ml of rPTN (R&D system, Minneapolis, MN). After 1–3 d of treatment, the cell viability was measured by a MTT assay kit (Promega, Madison, WI): The cells were plated in 96-well microtiter plates at a density of 5×10^3 cells per well and each plate was incubated for 24 h at 37°C in a CO2 (5%) incubator. Each well was washed with phosphate buffered saline (PBS) and incubated with rTGFβ1 in serum-free media for 1–3 d. The cells were counted with the kit according to the instructions provided by the manufacturer, and the absorbance of each well was measured at 450 nm with a microtiter plate reader. Apoptotic changes of nuclear chromatins were observed by staining cells with Hoechst 33342 (Wako): The cells were fixed with paraformaldehyde for 20 min and stained with Hoechst 33342 for 30 min, and 500 cells were counted in randomly chosen areas. The cells with condensed or fragmented nuclei were considered to be apoptotic and their occupancy was expressed as the percentage of apoptosis. TUNEL assay was also employed to confirm the cell death using an Apoptosis Detection Kit (Wako). Apoptosis was induced for normal rat hepatocytes as follows. The cells were maintained in DMEM containing 10% FBS for 1 d and were treated with 2 ng/ml of rTGFβ1 for 2 d. Hoechst staining was performed to detect the apoptosis as above.

Preparation of Hepatoma Cells That Constitutively Express PTN

Huh-7 cells were transfected with pcDNA3 vectors (Invitrogen, San Diego, CA) bearing PTN cDNA with Lipopectamine (Invitrogen), treated with Geneticin (Gibco) for 3 wk at 975 μg/ml concentration for selection. The selected single clones were plated in 24-well culture dishes, treated with trypsin, and collected. As a result, total 4 clones were selected, Huh-7-C2, -C4, -C5, and -C6, and used for further experiments. The expression of PTN in the clones was confirmed by RT-PCR and Western blotting analysis. Similarly, the Huh-7 cells were transfected with pcDNA3 vectors that did not bear the transgene and the obtained cells (Huh-7-V cells) were used as control cells.

Western Blotting for PTN, Poly ADP Ribose Polymerase, Caspase-8, and Caspase-3

rPTN was isolated as below from the media in which Huh-7-C4 and -C5 cells had been cultured for 3 d in the absence of TGFβ1. The collected media were passed through a heparin sepharose column (Biorad, Melville, NY). The absorbed proteins were dissolved in 2×-diluted sodium dodecyl sulfate (SDS) sample buffer consisting of 62.5 mM Tris–HCl (pH 6.8), 2% SDS, with or without 5% β-mercaptoethanol, 10% glycerol, and 0.002% bromophenol blue, and boiled for 5 min. The proteins were separated by 5–15% SDS–polyacrylamide gradient gel electrophoresis, transferred to nitrocellulose membranes (Schleicher & Schuell, Dassel, Germany), and were treated with anti-PTN antibodies (Santa Cruz). Enhanced chemiluminescence (Amersham) reagent was applied to visualize the protein bands. Standard rPTN was purchased from R&D system.

Huh-7-V, -C4, and -C5 cells were cultured for 3 d in the absence and the presence of 5 and 10 ng/ml TGFβ1 and were subjected to Western blotting for poly ADP ribose polymerase (PARP, a substrate of caspase-3 [27]), procaspase-8 and procaspase-3 as follows. Each of the above cells was dissolved in radioimmunoprecipitation (RIPA) buffer consisting of 50 mM Tris, pH 8.0, 150 mM NaCl, 0.1% SDS, 1% NP40, 1 mM phenylmethylsulfonyl fluoride (PMSF), and 1 μg/ml aprotinin. Soluble proteins were loaded on the polyacrylamide gels, and the blots were treated with antibodies against PARP (Zymed), caspase-8 (Santa Cruz), caspase-3 (Cell Signaling Technology, Beverly, MA), and actin (Santa Cruz). Fifty μM of Z-VAD-FMK (Promega) was treated to the Huh-7 cell before 1h of TGFβ1 treatment to inactivate the caspases. The intensity of the actin bands was utilized as a measure for equal loading.

Preparation of Hepatoma Cells Infected With Replication-Defective Recombinant Adenoviruses That Contain PTN Gene

Human PTN cDNA was inserted into replication-defective E1- and E3-adenoviral vectors containing the cytomegalovirus enhancer and the chicken β-actin promoter as a promoter. PTN-expressing adenovirus (PTN-Ad) was amplified in 293 kidney epithelial cells. The cells were disrupted by one cycle of freezing and thawing and centrifuged. PTN-Ad was obtained in the supernatant. Similarly, a vector of bacterial β-galactosidase (LacZ-Ad) was prepared as a control. Huh-7 and FaO cells were plated in 100 mm dishes and infected with 100 m.o.i. of PTN-Ad or LacZ-Ad for 4 h. The cells were trypsinized and plated at a density of 5×10^3 cells per well in 96-well plates.

Two days later, the cells were incubated in the absence or presence of TGFβ1 at 5 ng/ml for up to 2 or 3 d. The expression of PTN and β-galactosidase in the adenovirus-infected cells was confirmed by Western blotting with anti-PTN antibodies on the culture media and galactosidase staining on the infected cells, respectively.

Measurement of Caspase-3 Activity

Huh-7-V cells, Huh-7-C4, and -C5 cells were incubated in the absence or presence of TGFβ1 at 5 ng/ml for up to 3 d. Cell lysates were used for the measurement of the caspase-3 activity using a Caspase-Glo™ Assay kit (Promega) with a luminometer. The net activity of intracellular caspase-3 was calculated by the difference between samples incubated with or without TGFβ1. Similarly, the caspase-3 activity was determined for Huh-7 and FaO cells that had been transfected with PTN-Ad or LacZ-Ad.

Statistical Analysis

Numerical data are presented as the mean ± the standard deviation (SD) of independent determinations. Statistical analysis of differences was performed by Student's *t*-test, with a P value <0.05 being considered significant.

RESULTS

PTN mRNA Expression in Fibrotic Liver, Activated HSCs and Hepatoma Cells

Total RNAs were obtained from hepatoma HepG2, Huh-7, and FaO cells. hepatocytes and HSCs isolated from normal livers, HSCs (activated HSCs) from rats that had been treated with CCl_4 for 5 wk, and livers of rats treated with CCl_4 for 5 wk for measuring PTN mRNA expression levels by RT-PCR. PTN mRNA was undetectable in HepG2 and FaO cells, and in the normal hepatocytes (Figure 1A), but weakly detectable in Huh-7 cells, normal HSCs, and cirrhotic rat liver, and strongly expressed in the activated HSCs. These detected bands were not due to non-specific DNA amplification, because, sequencing of the each gave exactly the same sequence as the expected sequence (data not shown). α-SMA mRNA expression was markedly stimulated in HSCs from the CCl_4-treated rat liver compared to those from the control liver (Figure 1A), which confirmed the activation of HSCs by CCl_4-treatment. From these results we considered possible involvement of PTN in liver fibrogenesis and carcinogenesis.

Distribution of PTN Protein in CCl_4-Induced Fibrotic Liver

Rats were treated with CCl_4 for up to 10 wk and their livers were subjected to immunohistochemical examinations for PTN (Figure 1B). The CCl_4-treatment induced the formation of thick collagen fibers that formed fibrotic septa and the formation of hepatic nodules at 8 wk and thereafter (Figure 1B,c–f). PTN-positive (PTN^+) cells were detectable in nonparenchymal cells of the liver 5 wk post-CCl_4-treatment (Figure 1B,b), but not in the normal liver (Figure 1B,a). The positive cells increased the number as the CCl_4-treatment was prolonged to 8 wk (Figure 1B,c) and 10 wk (Figure 1B,d). The PTN^+-cells were largely in nonparenchymal regions, but some were in hepatic nodules that appeared 8 wk after the treatment (Figure 1B,e). The nodules observed at 10 wk post-treatment also contained the positive cells (Figure 1B,f). These results showed that nonparenchymal cells and hepatocytes in the nodules became PTN^+ during liver fibrosis.

Identification of PTN^+-Cells as Activated HSCs and Kupffer Cells

PTN^+-cells were immunohistochemically characterized. Rats were treated with CCl_4 for 8 wk, and their livers were subjected to double immunohistochemistry for PTN, α-SMA, and PTN, ED2. As shown in Figure 2A, the expression of α-SMA was significantly overlapped with that of PTN, suggesting that activated HSCs might be a major source of PTN-expression in the nonparenchymal cells of liver tissue. Double immunohistochemistry for PTN and ED2 revealed that some of the Kupffer cells also expressed PTN (Figure 2B). These results indicate that both activated HSCs and Kupffer cells express PTN during CCl_4 induced fibrogenesis.

PTN Inhibits TGFβ1-Induced Apoptosis in Huh-7 Hepatoma Cells

The above results strongly suggested the involvement of PTN in liver fibrogenesis. At first, we examined whether PTN shows growth promoting activity on hepatocytes. Huh-7 cells, HepG2 cells, and normal rat hepatocytes were cultured for 1 wk in the presence of rPTN (Figure 3A). PTN increased proliferation of both HepG2 cells and normal rat hepatocytes, but not that of Huh-7 cells. Huh-7 cells, but not HepG2 and normal rat hepatocytes weakly expressed PTN mRNA (Figure 1A), which led us to consider that exogenous PTN was not effective in the proliferation of Huh-7 cells. Next, we examine the role of PTN in hepatic fibrogenesis in relation to the role of TGFβ1, because there have been abundant studies that showed the involvement of TGFβ1 in the pathological process of liver fibrosis [28,29]. We tested the role of PTN in TGFβ1-induced apoptosis in carcinogenesis using Huh-7 cells, because these cells have been known to be sensitive to TGFβ1 in which TGFβ1 induces the apoptosis through activating caspases [24]. Huh-7 cells were co-treated with rPTN (100 ng/ml) and rTGFβ1 (1 and 2 ng/ml) for up to 3 d. The cell number was determined during the culture period (Figure 3B). rTGFβ1 decreased the cell number in a dose-dependent manner. The presence of rPTN in the culture antagonized this action of rTGFβ1. But

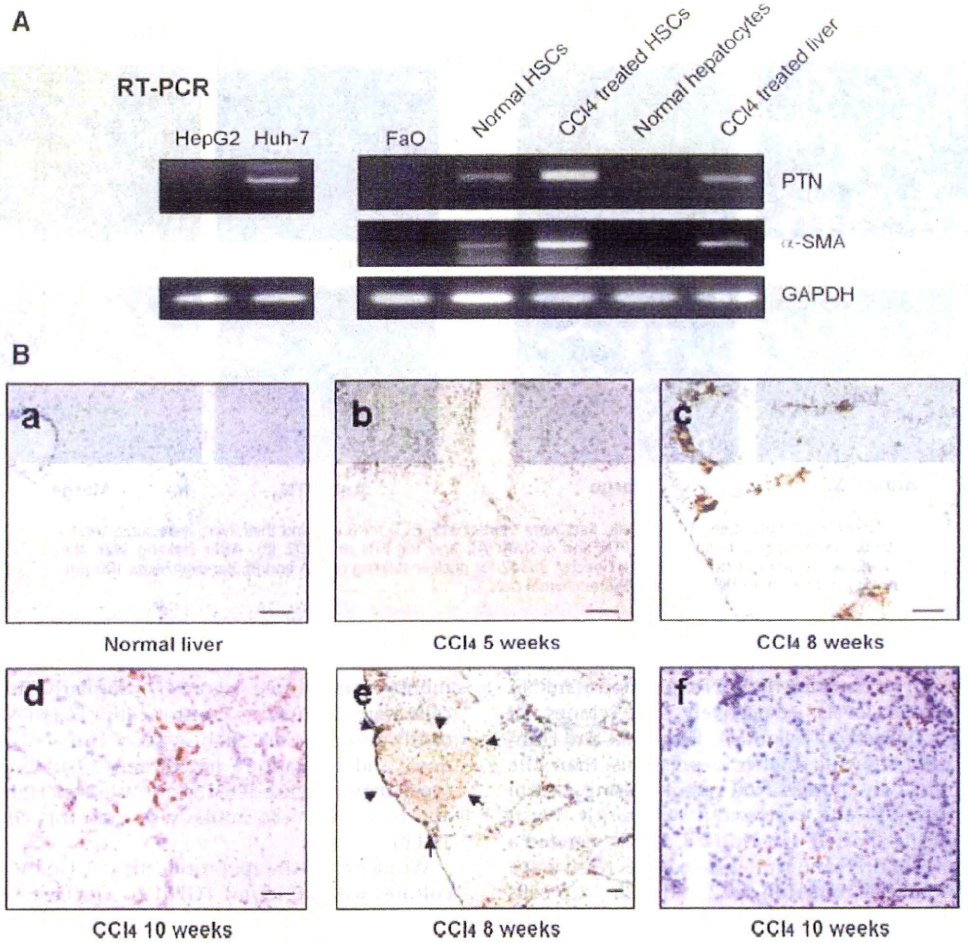

Figure 1. Expression of PTN mRNA and protein. (A) PTN and α-SMA mRNA expression. Total RNA was isolated from HepG2 and Huh-7 cells and subjected to RT-PCR amplification of PTN, α-SMA and GAPDH cDNAs in one series of experiment (left panel) and from FaO cells, HSCs and hepatocytes from normal liver, HSCs from CCl_4-treated liver, and CCl_4-treated liver in another series of experiment (right panel). (B) Distribution of PTN in CCl_4-treated liver. Rats were treated with mineral for 10 d (a), or with CCl_4 for 5 (b), 8 (c and e), and 10 wk (d and f), and their livers were subjected to immunohistochemistry with anti-PTN antibodies. (a) There is no PTN^+-cells. (b) There are a few PTN^+-cells in the nonparenchymal cells. (c) PTN^+-cells are often distributed in the nonparenchymal cells. (d) Distribution of PTN^+-cells is similar as in c. (e) A nodule is positive for PTN. (f) A nodule is positive for PTN. Arrows in e indicate the PTN^+-liver nodule. Bar represents 100 μm.

when treated with more than 5 ng/ml of TGFβ1, the cells were unable to escape from the apoptosis even in the presence of PTN (data not shown). The cells were stained with Hoechst 33342 and examined for the presence of chromosomal condensations (Figure 3C). TGFβ1 evidently induced the apoptotic changes of chromatin. The frequency of cells with such changes was counted on the photographs (Figure 3D). rTGFβ1 at 2 ng/ml increased the apoptosis rate >3-fold compared to that of the control cells. The presence of rPTN at 100 ng/ml significantly decreased the rTGFβ1-stimulated level to <50%. These results support the previous report that TGFβ1 enhances the apoptosis of Huh-7 cells [24]. Identical experiments were undertaken using normal rat hepatocytes (Figure 3E and F). Although the induction rate was less than in Huh-7 cells, TGFβ1 at 2 ng/ml also induced the apoptotic change in chromatin, which was significantly inhibited by PTN.

Establishment of PTN Gene-Expressing Huh-7 Cells

To further investigate the anti-"TGFβ1-induced apoptotic function" of PTN, we established a PTN gene-expressing Huh-7 cell line. RT-PCR showed that Huh-7 cells themselves weakly expressed PTN mRNA, but its proteins were undetectable by Western blotting (Figure 4A). We transfected pcDNA3-PTN to Huh-7 cells and selected out the single cell colonies designated Huh-7-C2, -C4, -C5, and -C6 as

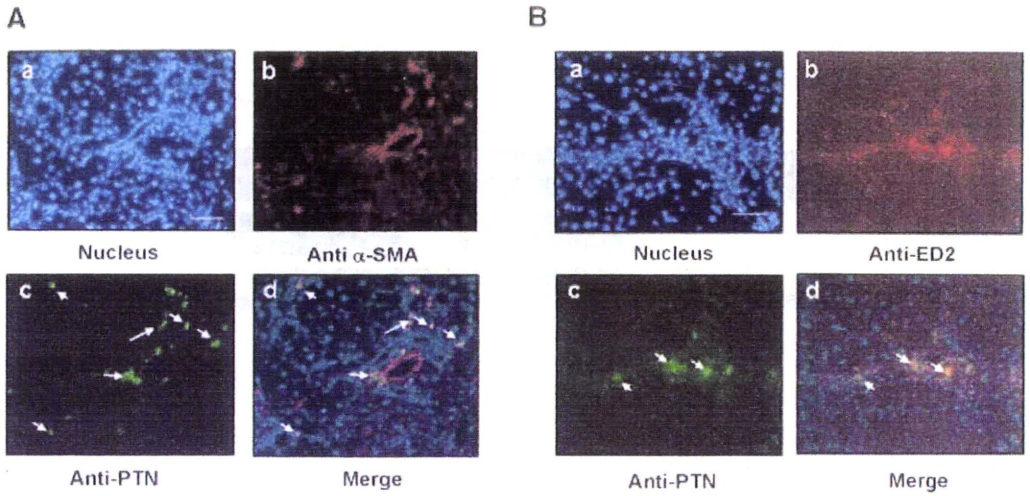

Figure 2. Identification of PTN^+-cells. Rats were treated with CCl_4 for 8 wk, and their livers were subjected to double immunohistochemistry for PTN and α-SMA (A), and for PTN and ED2 (B). After staining with the antibodies sections were stained with Hoechst 33342 for nuclear staining (a in A and B). Bar represents 100 μm. Arrows indicate the PTN positive nonparenchymal cells.

Geneticin-resistant colonies. These cells were subjected to RT-PCR (Figure 4A) and Western blotting (Figure 4B) for checking the PTN expression at mRNA and protein levels, respectively. The clones all strongly expressed PTN mRNA, Huh-7-C4 and Huh-7-C5 cells showing higher expressions than the remaining two colonies. Null vector-bearing control cells, Huh-7-V cells, expressed it very faintly. Western blotting showed that Huh-7-C5 cells secreted a high level of rPTN and Huh-7-C4 cells secreted it at a detectable level, but Huh-7-C2 and Huh-7-C6 cells did not.

Effects of TGFβ1 on Apoptosis of PTN Gene-Expressing Huh-7 Cells

First we found that there was no significant difference in the proliferate ability between PTN gene-expressing (Huh-7-C4 and Huh-7-C5) and control cells (Huh-7-V cells) (Figure 4C). Next, we evaluated the TGFβ1 effect on the PTN transfected cells: Huh-7-C4 and Huh-7-C5 cells were cultured for up to 3 d in the presence of three different concentrations of TGFβ1 (1, 5, and 10 ng/ml) and the cell number was counted (Figure 4D). Similarly, Huh-7-V cells were cultured as control cells. TGFβ1 significantly decreased the cell number of Huh-7-V cells in dose- and the culture length-dependent manners (open bars in Figure 4D). In contrast, Both Huh-7-C4 and Huh-7-C5 cells similarly resisted this effect of TGFβ1.

We identified the apoptotic cells at 3 d in the above cultures with 10 ng/ml TGFβ1 by Hoechst- (Figure 4E,a and c) and TUNEL-staining (Figure 4E,d and f). It was apparent that TGFβ1-induced apoptotic cells were significantly decreased in both Huh-7-C4 (Figure 4E,b and e) and -C5 (Figure 4E,c and f) compared to the control cells (Figure 4E,a and d). The number of the apoptotic cells was counted for each of the TUNEL-stained cells and their incidence is shown in Figure 4F. The ratio of apoptotic cells in both clones bearing PTN-genes was decreased to approximately 25% of the control cells.

Figure 3. (*Overlesf*) Suppression of TGFβ-induced apoptosis in hepatoma cells by PTN. (A) Effects of PTN on the growth of cells of cancer cell line and normal hepatocytes. Cells of Huh-7, HepG2, and primary rat hepatocytes, 5×10^3 cells each, were seeded in 12 well plates and treated with 100 ng/ml of rPTN for 1 wk. rPTN increased the proliferation of HepG2 cells and normal rat hepatocytes, but not Huh-7 cells. The same experiment was repeated 3 times and the results are presented as the mean ± SD. (B) The effects of PTN on the cell viability. Huh-7 cells were treated with 0, 1, and 2 ng/ml of rTGFβ1 with or without 100 ng/ml of rPTN for up to 3 d. The number of the cells was counted at 2 and 3 d in culture and the results are shown as % of the number of the cells that had no treatment. The open bars represent the cultures in the presence of TGFβ1 at the indicated concentrations, but in the absence of rPTN. The closed bars are for the cultures in the presence of both TGFβ1 and rPTN. (C) Apoptotic changes in nuclear chromatins of Huh-7 cells. The cells at 2 d with 2 ng/ml TGFβ1 and 100 ng/ml rPTN each alone or together shown in (B) were stained with Hoechst 33342 to examine the apoptotic changes in nuclear chromatins. (a) Cells without cytokines. (b) Cells with 2 ng/ml TGFβ1. (c) Cells with 100 ng/ml rPTN. (d) Cells with both 2 ng/ml TGFβ1 and 100 ng/ml rPTN. Bar represents 100 μm. (D) The incidences of apoptosis of the cultured Huh-7 cells. The number of the apoptotic cells was counted in (C) and divided by the total cells in the tested field to obtain the apoptosis rate (%). "No Tx" represents the cells without treatment. * represents the statistical significance at $P < 0.05$ between "TGFβ1" and "PTN and TGFβ1". (E) Apoptotic changes in nuclear chromatins of normal rat hepatocytes. The cells at 2 d with 2 ng/ml TGFβ1 and 100 ng/ml rPTN each alone or together were stained with Hoechst 33342 as in (C). (a) Cells without cytokines. (b) Cells with 2 ng/ml TGFβ1. (c) Cells with 100 ng/ml rPTN. (d) Cells with both 2 ng/ml TGFβ1 and 100 ng/ml rPTN. Bar represents 100 μm. (F) The incidences of apoptosis of the rat hepatocytes. The apoptosis rate (%) was calculated as in (D). * represents the statistical significance at a $P < 0.05$ level between TGFβ1 treatment versus TGFβ1 and rPTN co-treatment.

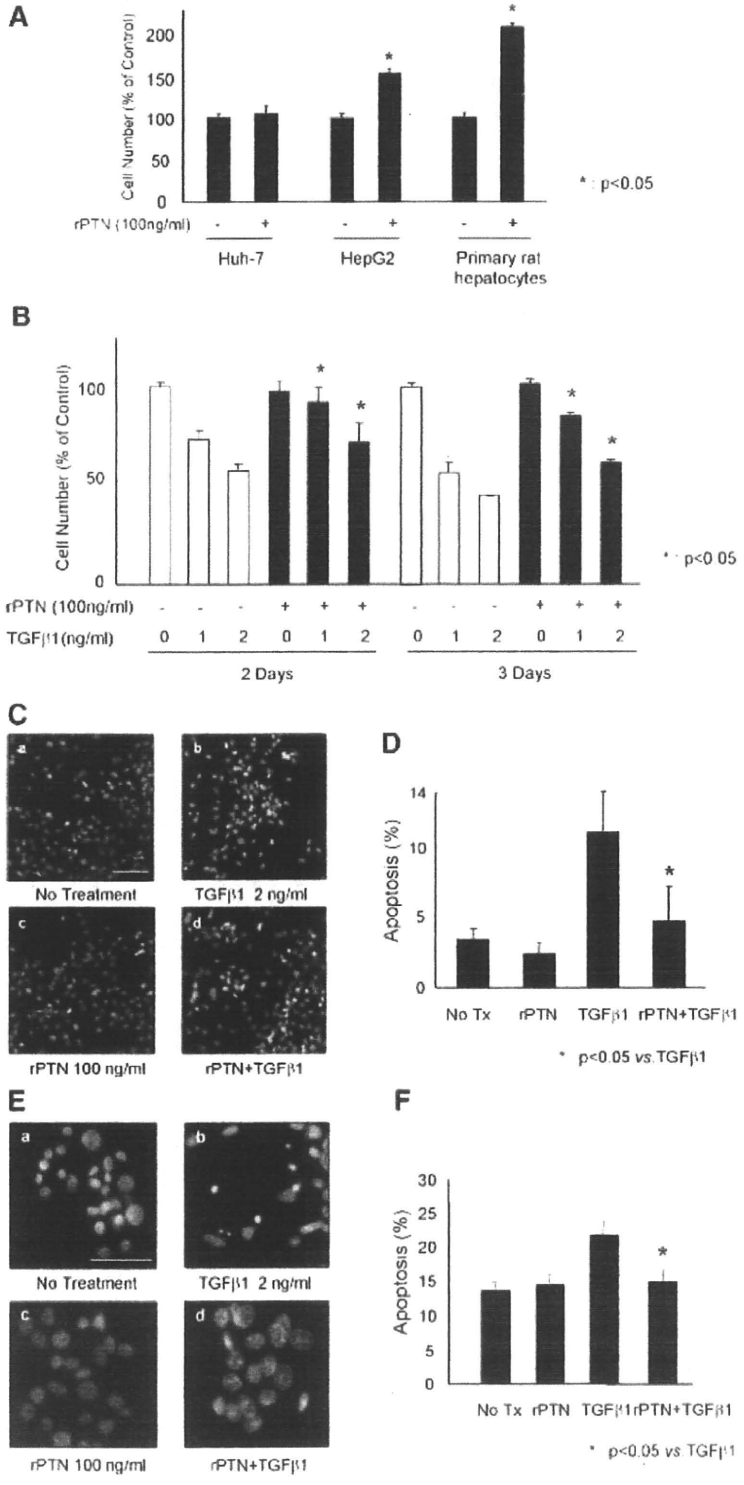
A
Cell Number (% of Control)
200
150
100
50
0
rPTN (100ng/ml) - + - + - +
Huh-7
HepG2
Primary rat hepatocytes
* : p<0.05
B
Cell Number (% of Control)
100
50
0
rPTN (100ng/ml) - - - + + + - - - + + +
TGFβ1(ng/ml) 0 1 2 0 1 2 0 1 2 0 1 2
2 Days
3 Days
* : p<0 05
C
a
b
No Treatment
TGFβ1 2 ng/ml
c
d
rPTN 100 ng/ml
rPTN+TGFβ1
D
Apoptosis (%)
14
10
5
0
No Tx
rPTN
TGFβ1
rPTN+TGFβ1
* p<0.05 vs TGFβ1
E
a
b
No Treatment
TGFβ1 2 ng/ml
c
d
rPTN 100 ng/ml
rPTN+TGFβ1
F
Apoptosis (%)
30
25
20
15
10
5
0
No Tx
rPTN
TGFβ1
rPTN+TGFβ1
* p<0.05 vs TGFβ1

Figure 3.

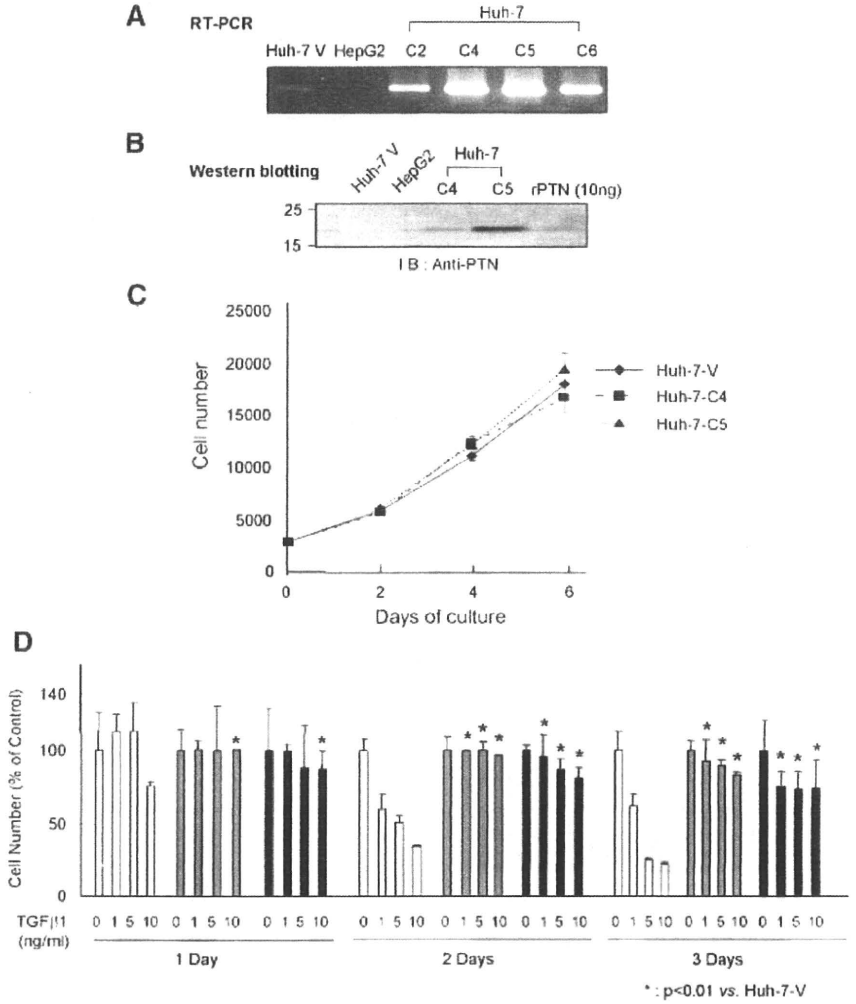

Figure 4. Effects of TGFβ1 on PTN-expressing Huh-7 cells. (A) Establishment of PTN gene-expressing Huh-7 cells. Huh-7 cells were transfected with pcDNA3 vectors bearing PTN cDNA, which yielded four single cell colonies, Huh-7-C2, Huh-7-C4, Huh-7-C5, and Huh-7-C6. Expression levels of PTN mRNA and protein were determined by RT-PCR (A) and Western blotting (B), respectively. Similarly, the expression levels were determined for Huh-7-V and HepG2 cells. Huh-7-V cells weakly expressed PTN mRNA, but HepG2 cells did not. Huh-7-C2, -C4, -C5, and -C6 expressed PTN mRNA, but only Huh-7-C4 and Huh-7-C5 cells secreted PTN protein in culture media at detectable levels. The molecular masses are shown at the left side of the gel. The most right lane was for 10 ng of standard rPTN. (C) Growth of PTN gene-expressing Huh-7 cells. Huh-7-V, Huh-7-C4, and Huh-7-C5, 3×10^3 cells each, were seeded in 24-well plates and cultured for 6 d. Cells were harvested at 2, 4, and 6 d of culture for cell count. The same experiment was repeated 3 times and the results are presented as the mean ± SD. (D) Effects of TGFβ1 on PTN-expressing Huh-7 cells. Huh-7-V, -C4, and -C5 cells were cultured up to 3 d in the presence of 0, 1, 5, and 10 ng/ml. The cell number was counted at 1, 2, and 3 d in culture and the cell number ratio (%) was calculated as in Figure 3B. The open, gray, and black bars represent Huh-7-V, -C4, and -C5 cells, respectively. * represents the statistical significance at a $P < 0.01$ level between Huh-7-V versus Huh-7-C4 and -C5 cells. (E) Identification of apoptotic cells in cultures. Huh-7-V (a and d), -C4 (b and e), and -C5 cells (c and f) were cultured for 3 d in the presence of 10 ng/ml TGFβ1 and stained with Hoechst (a–c) or with TUNEL (d–f). Bar represents 100 μm. (F) The apoptotic cell ratio was determined by dividing the number of the $TUNEL^+$-cells with that of the total number in the examined field. Each number was obtained from photos shown in (E,d–f). * represents the statistical significance at a $P < 0.01$ level between Huh-7-V versus Huh-7-C4 and -C5 cells. (G) The cell viability in the presence of mitomycin C. Huh-7-V, -C4, and -C5 cells were cultured for 2 d as in C except that TGFβ1 was replaced with mitomycin C at the indicated concentrations. The three differently colored bars represent cell species as in (C). (H) Suppression of TGFβ1-induced apoptosis in Huh-7-C5 conditioned media. Huh-7-V and Huh-7-C5 cells, 5×10^5 cells each, were seeded in 100 mm dishes and cultured for 2 d. The culture media were collected and used as the conditioned media. Huh-7 cells were cultured in the conditioned media from Huh-7-C5 or Huh-7-V in the presence of 2 ng/ml TGFβ1. CM: conditioned media. (I) The incidences of apoptosis of the Huh-7 cell. The number of the apoptotic cells was counted on photographs shown H and the apoptosis rate (%) was obtained as in E.

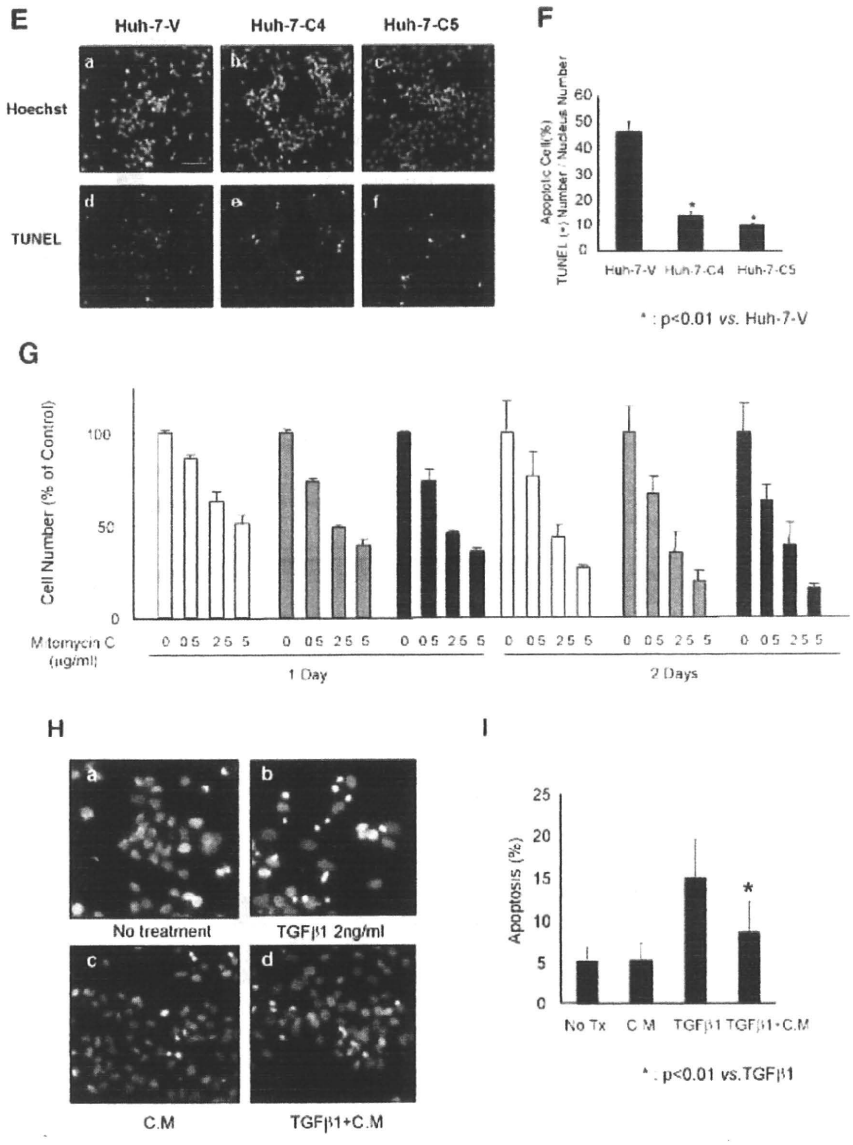

Figure 4. (*Continued*)

In order to exclude the possibility that this anti-apoptotic effect of PTN is a merely non-specific action, we induced the apoptosis on each of these cells with mitomycin-C at concentrations from 0.5 to 5 μg/ml and examined the change in cell number as a measure of apoptosis (Figure 4G). There were no differences in the rate of the cell number decrease among the cells, indicating that PTN specifically inhibit TGFβ1-mediates cell death. The results strongly suggested that PTN secreted by PTN gene-expressing Huh-7 cells suppresses the TGFβ1-induced apoptosis. To further test this suggestion, we examined the effect of conditioned media from the Huh-7-C5 on the TGFβ1-induced apoptosis. Huh-7 cells were cultured in the conditioned media in the presence of 2 ng/ml of TGFβ1 for 3 d. Hoechst staining showed that the conditioned medium apparently inhibited the TGFβ1-induced apoptosis (Figure 4H), which was supported by the quantitative analysis in which the number of the apoptotic cells was counted on the photographs in Figure 4H to calculate the incidence of apoptosis (Figure 4I).

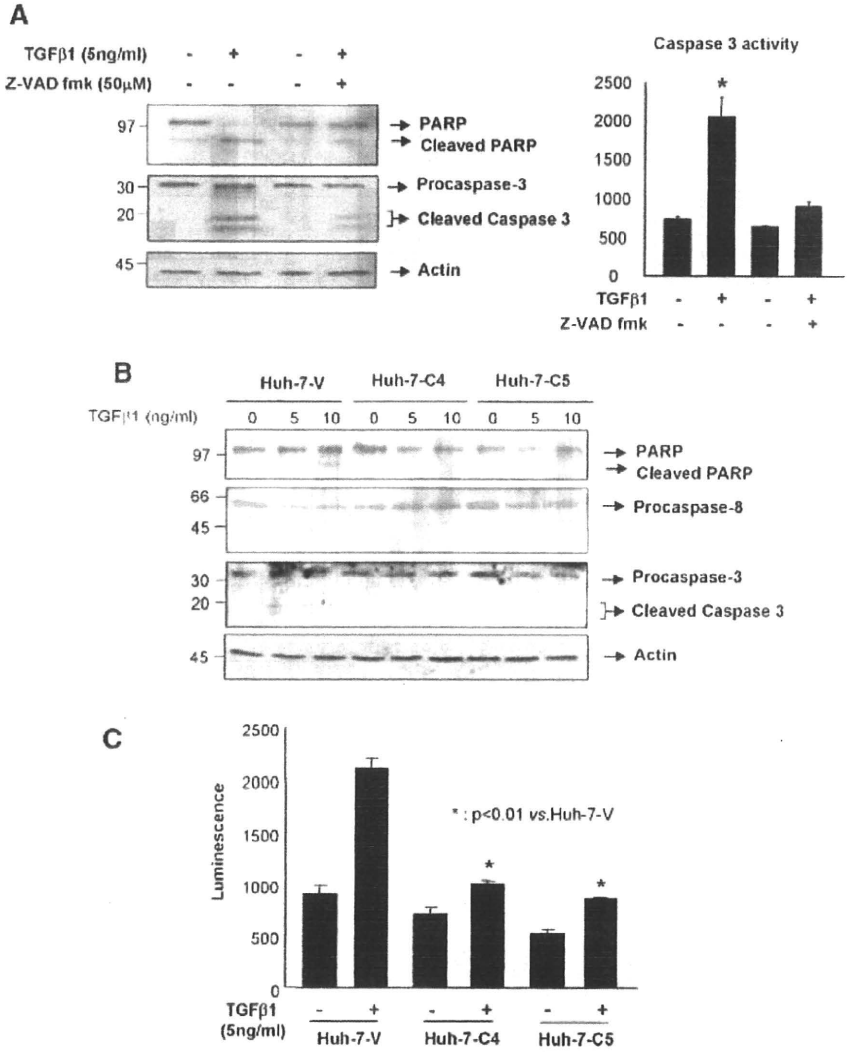

Figure 5. Suppression of TGFβ1-induced activation of caspase-8 and caspase-3 by PTN. (A) Activation of caspase-3 by TGFβ1 in Huh-7 cells. The cells were cultured in the absence (–) or presence (+) of 5 ng/ml TGFβ1 and 50 μM Z-VAD-FMK for 3 d. The cell lysates were prepared from each of the cultured cells and subjected to Western blotting for PARP and procaspase-3 (left panel) and to measurement of caspase-3 activity (right panel). The Arabic numerals at the left side of the gel represent molecular masses. (B) Suppression of TGFβ1-induced cleavage of cellular PARP, pro-caspase-8, and pro-caspase 3 in PTN gene-expressing Huh-7 cells. Huh-7-V, -C4, and -C5 cells were cultured for 3 d in the absence and the presence of 5 and 10 ng/ml TGFβ1. The whole cell lysates of each of the cells was subjected to Western blotting for PARP, caspase-8, caspase-3, and actin. (C) Suppression of TGFβ1-induced caspase-3 activity in Huh-7 cells bearing PTN gene. The whole lysates of the cells in B were used for determining the caspase-3 activity. * represents the statistical significance at $P < 0.01$ level between TGFβ1 treated Huh-7-V versus TGFβ1-treated Huh-7-C4 and -C5 cells.

Inhibition of TGFβ1-Induced Caspase-3 Activation by PTN

The activation of caspase cascades has been known as an essential molecular event in the TGFβ1-induced apoptosis [24]. We investigated an aspect of the mechanism of PTN action on TGFβ1-induced apoptosis targeting the caspase activation. First, we examined the activation of caspase-3 by TGFβ1 in Huh-7 cells (Figure 5A). The cells were cultured in the absence or presence of 5 ng/ml TGFβ1 and Z-VAD-FMK, a caspase inhibitor, for 3 d. The cell lysates were subjected to Western blotting for PARP and procaspase-3 (Figure 5A, left panel). The bands corresponding to the cleaved products of PARP and procaspase-3 were clearly visible. The caspase-3 activity was measured in the cell lysates (Figure 5A, right panel), which quantitatively demonstrated that rTGFβ1 stimulated the activity and Z-VAD-FMK suppressed the rTGFβ1-induced activity.

We examined the TGFβ1-induced apoptosis in PTN-expressing Huh-7 cells. Huh-7-V, Huh-7-C4, and -C5 cells were cultured in the presence of TGFβ1 for 3 d and their cell lysates were Western blotted for PARP, capase-8, and -3 (Figure 5B). rTGFβ1 also induced the cleavage of PARP, procaspase-8 and procaspase-3 in Huh-7-V cells. However, there were no such processed products in Huh-7-C4 and -C5 cells. Actually, the treatment of Huh-7-V cells with rTGFβ1 enhanced the caspase-3 activity (Figure 5C). The extent of the activation was much less in Huh-7-C4 and -C5 cells, supporting the idea that PTN has the suppressive activity on TGFβ1-induced apoptosis.

The anti-apoptotic function of PTN was further tested using FaO rat hepatoma cells, which are also highly sensitive to TGFβ1 in apoptosis induction [30]. Both FaO and Huh-7 cells were transduced with adenovirus vectors carrying PTN gene (PTN-Ad). It was shown that these cells secreted PTN proteins in culture media (Figure 6A). The cells were then treated with 5 ng/ml rTGFβ1 for 2 or 3 d. As shown in Figure 6B and C both types of cells became reluctant to activate caspase-3 in response to TGFβ1 when transfected with PTN gene. These results strongly support that PTN suppresses TGFβ1-induced caspase 3 activation and apoptosis.

DISCUSSION

Studies abundantly accumulated hitherto indicate that the signaling between hepatocytes and HSCs plays a crucial role in regulating normal and abnormal growth of hepatocytes [31]. Especially the role of HSCs in the hepatic fibrogenesis and carcinogenesis has been a major issue among investigators [32]. Previously, we showed that HSC-derived PTN plays a role as a hepatocytes growth factor [6,9]. Furthermore, we showed that PTN

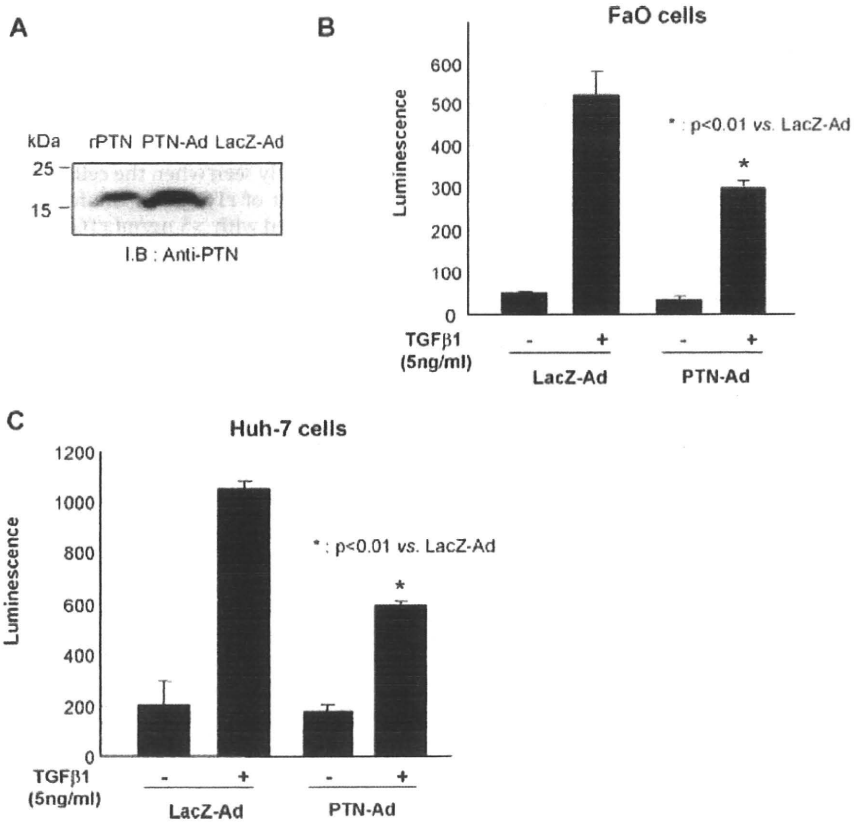

Figure 6. Reluctance of PTN-transgenic cells in responding to TGFβ1. FaO and Huh-7 cells were exposed to PTN- or LacZ-Ad for 3 d and then treated with TGFβ1. (A) Expression of rPTN proteins by the transgenic cells. The culture media were collected from the cell cultures and passed through a heparin gel column. The absorbed proteins were Western blotted with antibodies against PTN. Left, middle, and right lanes were for standard rPTN (10 ng), FaO cells transfected with PTN-Ad, and those with LacZ-Ad, respectively. (B) Suppression of TGFβ1-induced caspase-3 activation in the FaO cells bearing PTN-Ad. The whole lysates were prepared from the above cells for measuring the caspase-3 activity. The symbols, – and +, indicate the absence and presence of 5 ng/ml TGFβ1. (C) Suppression of TGFβ1-induced caspase-3 activation in the Huh-7 cells bearing PTN-gene. Caspase-3 activity was measured for Huh-7 cells as in B. * represents the statistical significance at a $P < 0.01$ level between TGFβ1-treated FaO or Huh-7 cells with LacZ-Ad versus TGFβ1-treated FaO or Huh-7 cells with PTN-Ad.

expression was increased in CCl_4-induced fibrotic liver [10], suggesting the involvement of PTN in hepatic fibrogenesis, to which TGFβ1 is also committed as an anti-hepatocyte growth factor and an ECM-formation accelerator. These previous studies were the major motivation of the present study and we investigated the mechanism of the action of PTN in liver fibrogenesis and carcinogenesis. As a result, we confirmed the previous studies that HSCs and also hepatocytes later increased PTN mRNA expressions during CCl_4-induced liver fibrosis. This confirmation strengthens the previous suggestion that PTN plays a role in liver fibrogenesis.

In this study the role of PTN in hepatic carcinogenesis was tested utilizing known TGFβ1-sensitive human and rat hepatoma cells, Huh-7 and FaO cells, respectively. These cells undergo apoptosis when stimulated by TGFβ1 [30]. We were able to demonstrate that PTN acts as an anti-apoptotic factor. Interestingly, this activity appears to be specific to the TGFβ1-induced apoptosis, because PTN did not show any effect on mitomycin C-induced hepatocyte apoptosis. Caspase-3 is known as a main executor of cell death [33]. It is most likely that PTN suppresses the activation of caspase-8 and cannot activate the caspase-3. We noticed that the extent of the suppression of caspase-3 activity in PTN-Ad-bearing Huh-7 cells (Figure 6C) was lower than that in Huh-7-C4 and -5 (Figure 5C). The PTN-expression by the former cells was transient, peaking at 3 d after infection and was terminated at 7 d (data not shown). In the experiment with PTN-Ad-bearing Huh-7 cells, the cells were treated with TGFβ1 for 3 d from 3 to 6 d post-infection, during which the PTN expression level was considered to be apparently much decreased. This decrease might explain the difference between the suppression levels in the two experiments.

Such an anti-apoptotic effect of PTN appears to be important in hepatocarcinogenesis, because chemically altered hepatocytes undergo the apoptotic pathway through the action of several cytokines in the process of carcinogenesis. It is conceivable that transformed hepatocytes exposed to TGFβ1 are on the two possible paths, one for undergoing apoptosis and the other for escaping from the apoptosis. It is suggested that the cells are capable of "successfully" escaping from the TGFβ1-induced apoptosis under a "favorable" signal such as PTN in this case. Such possibility has earlier been investigated in the chemically induced carcinogenesis in rat liver [21].

TGFβ1 has been shown to be an inhibitor of hepatocyte proliferation as well as a potent inducer of apoptosis in vitro and in vivo, when administered at a high dose, thus indicating that this cytokine can induce regression of rat livers [34,35]. The level of TGFβ1 in liver and serum is increased in the chemically induced liver cirrhosis and carcinogenesis in humans as well as rats [21]. Blocking of TGFβ1 by TGFβ1 type II receptor dominant negative or TGFβ1 soluble antibodies inhibits the fibrosis in dimethylnitrosamine-induced liver fibrosis [19,36]. Furthermore, the hepatocyte proliferation was enhanced in the absence of TGFβ type II receptor in chemically induced hepatocarcinogenesis [21]. Several studies suggest that TGFβ1 is a potent activator of hepatocyte apoptosis and the loss of TGFβ1 signal activates hepatocyte proliferation and hepatocarcinogenesis. These studies all suggest TGFβ1 as one of the potent apoptotic factors working in liver fibrogenesis and carcinogenesis. We propose from the results obtained in the present study that PTN plays a role to protect transforming hepatocytes from apoptosis by suppressing the activity of TGFβ1. However, the effect of PTN on the promoting activity of ECM production, another major activity of TGFβ1, during liver fibrogenesis and carcinogenesis was not tested in the present study and remains to be clarified.

We showed the anti-apoptosis activity of PTN in two different experiments: one was that both rPTN and rTGFβ1 were introduced in cultures of Huh-7 cells with different concentration combinations and the other was that rTGFβ1 was introduced at various concentrations in culture media of PTN-gene transgenic Huh-7 and FaO cells. Anti-apoptotic effect of rPTN was only seen when the cells were treated with in <5 ng/ml of rTGFβ1 in the former experiment. When treated with >5 ng/ml rTGFβ1, the cells were unable to escape from the apoptosis. Furthermore, the effective inhibition of the apoptosis was seen when the concentration of rPTN was >100 ng/ml (data not shown). This might be partly a reflection of the instability of rPTN in the culture media. PTN gene-expressing cell lines were more resistant against the TGFβ1-induced apoptosis. The activation of procaspase-3 did not occur in these cells even at 10 ng/ml of rTGFβ1. Furthermore, PTN-Ad also protected Huh-7 and FaO cells from TGFβ1-induced apoptosis at 5 ng/ml of rTGFβ1. These results indicate that the continuous presence of PTN is more effective than its transient presence.

The present study has made two contributions to the understanding of biological roles of PTN. Firstly, in this study we show that PTN is largely expressed in HSCs and Kupffer cells, and also in some of hepatocytes during liver fibrosis. Secondly, the presence of PTN makes cells resistant to TGFβ1-induced cell death through the inhibition of caspase 3 activation. In summary, PTN is involved in hepatocarcinogenesis and has an anti-apoptotic activity against TGFβ1.

ACKNOWLEDGMENTS

This work was supported by grants from Hiroshima University 21st Century COE Program and CLUSTER, Japan, and was supported by the 2006 grant from Ajou University School of Medicine.

REFERENCES

1. Deuel TF, Zhang N, Yeh HJ, Silos-Santiago I, Wang ZY. Pleiotrophin: A cytokine with diverse functions and a novel signaling pathway. Arch Biochem Biophys 2002;397:162–171.
2. Milner PG, Li YS, Hoffman RM, Kodner CM, Siegel NR, Deuel TF. A novel 17 kD heparin-binding growth factor (HBGF-8) in bovine uterus: Purification and N-terminal amino acid sequence. Biochem Biophys Res Commun 1989;165: 1096–1103.
3. Li YS, Milner PG, Chauhan AK, et al. Cloning and expression of a developmentally regulated protein that induces mitogenic and neurite outgrowth activity. Science 1990; 250:1690–1694.
4. Kadomatsu K, Tomomura M, Muramatsu T. cDNA cloning and sequencing of a new gene intensely expressed in early differentiation stages of embryonal carcinoma cells and in mid-gestation period of mouse embryogenesis. Biochem Biophys Res Commun 1988;151:1312–1318.
5. Laaroubi K, Delbe J, Vacherot F, et al., Mitogenic and in vitro angiogenic activity of human recombinant heparin affin regulatory peptide. Growth Factors 1994;10:89–98.
6. Asahina K, Sato H, Yamasaki C, et al. Pleiotrophin/heparin-binding growth-associated molecule as a mitogen of rat hepatocytes and its role in regeneration and development of liver. Am J Pathol 2002;160:2191–2205.
7. Chauhan AK, Li YS, Deuel TF. Pleiotrophin transforms NIH 3T3 cells and induces tumors in nude mice. Proc Natl Acad Sci USA 1993;90:679–682.
8. Chen H, Gordon MS, Campbell RA, et al. Pleiotrophin is highly expressed by myeloma cells and promotes myeloma tumor growth. Blood 2007;110:287–295.
9. Sato H, Funahashi M, Kristensen DB, Tateno C, Yoshizato K. Pleiotrophin as a Swiss 3T3 cell-derived potent mitogen for adult rat hepatocytes. Exp Cell Res 1999;246:152–164.
10. Kohashi T, Tateaki Y, Tateno C, Asahara T, Obara M, Yoshizato K. Expression of pleiotrophin in hepatic non-parenchymal cells and preneoplastic nodules in carbon tetrachloride-induced fibrotic rat liver. Growth Factors 2002;20:53–60.
11. Hsu IC, Metcalf RA, Sun T, Welsh JA, Wang NJ, Harris CC. Mutational hotspot in the p53 gene in human hepatocellular carcinomas. Nature 1991;350:427–428.
12. Moriya K, Fujie H, Shintani Y, et al. The core protein of hepatitis C virus induces hepatocellular carcinoma in transgenic mice. Nat Med 1998;4:1065–1067.
13. Thorgeirsson SS, Teramoto T, Factor VM. Dysregulation of apoptosis in hepatocellular carcinoma. Semin Liver Dis 1998; 18:115–122.
14. Bataller R, Brenner DA. Liver fibrosis. J Clin Invest 2005;115: 209–218.
15. Miwa Y, Harrison PM, Farzaneh F, Langley PG, Williams R, Hughes RD. Plasma levels and hepatic mRNA expression of transforming growth factor-beta1 in patients with fulminant hepatic failure. J Hepatol 1997;27:780–788.
16. Carr BI, Hayashi I, Branum EL, Moses HL. Inhibition of DNA synthesis in rat hepatocytes by platelet-derived type beta transforming growth factor. Cancer Res 1986;46:2330–2334.
17. Strain AJ, Frazer A, Hill DJ, Milner RD. Transforming growth factor beta inhibits DNA synthesis in hepatocytes isolated from normal and regenerating rat liver. Biochem Biophys Res Commun 1987;145:436–442.
18. Caja L, Ortiz C, Bertran E, et al. Differential intracellular signaling induced by TGF-beta in rat adult hepatocytes and hepatoma cells: Implications in liver carcinogenesis. Cell Signal 2007;19:683–694.
19. Nakamura T, Sakata R, Ueno T, Sata M, Ueno H. Inhibition of transforming growth factor beta prevents progression of liver fibrosis and enhances hepatocyte regeneration in dimethylnitrosamine-treated rats. Hepatology 2000;32: 247–255.
20. Park YN, Chae KJ, Kim YB, Park C, Theise N. Apoptosis and proliferation in hepatocarcinogenesis related to cirrhosis. Cancer 2001;92:2733–2738.
21. Lim IK, Park SC, Song KY, et al. Regulation of selection of liver nodules initiated with N-nitrosodiethylamine and promoted with nodularin injections in fischer 344 male rats by reciprocal expression of transforming growth factor-beta1 and its receptors. Mol Carcinog 1999;26:83–92.
22. Fan G, Ma X, Kren BT, Steer CJ. The retinoblastoma gene product inhibits TGF-beta1 induced apoptosis in primary rat hepatocytes and human HuH-7 hepatoma cells. Oncogene 1996;12:1909–1919.
23. Black D, Lyman S, Qian T, et al. Transforming growth factor beta mediates hepatocyte apoptosis through Smad3 generation of reactive oxygen species. Biochimie 2007;89: 1464–1473.
24. Shima Y, Nakao K, Nakashima T, et al. Activation of caspase-8 in transforming growth factor-beta-induced apoptosis of human hepatoma cells. Hepatology 1999;30:1215–1222.
25. Tateno C, Takai-Kajihara K, Yamasaki C, Sato H, Yoshizato K. Heterogeneity of growth potential of adult rat hepatocytes in vitro. Hepatology 2000;31:65–74.
26. Kristensen DB, Kawada N, Imamura K, et al. Proteome analysis of rat hepatic stellate cells. Hepatology 2000; 32: 268–277.
27. Tewari M, Quan LT, O'Rourke K, et al. Yama/CPP32 beta, a mammalian homolog of CED-3, is a CrmA-inhibitable protease that cleaves the death substrate poly(ADP-ribose) polymerase. Cell 1995;81:801–809.
28. Czaja MJ, Weiner FR, Flanders KC, et al. In vitro and in vivo association of transforming growth factor-beta 1 with hepatic fibrosis. J Cell Biol 1989;108:2477–2482.
29. Armendariz-Borunda J, Seyer JM, Kang AH, Raghow R. Regulation of TGF beta gene expression in rat liver intoxicated with carbon tetrachloride. FASEB J 1990;4: 215–221.
30. Lim IK, Joo HJ, Choi KS, et al. Protection of 5alpha-dihydrotestosterone against TGF-beta-induced apoptosis in FaO cells and induction of mitosis in HepG2 cells. Int J Cancer 1997;72:351–355.
31. Gressner AM, Lahme B, Brenzel A. Molecular dissection of the mitogenic effect of hepatocytes on cultured hepatic stellate cells. Hepatology 1995;22:1507–1518.
32. Lissoos TW, Davis BH. Pathogenesis of hepatic fibrosis and the role of cytokines. J Clin Gastroenterol 1992;15:63–67.
33. Nicholson DW, Ali A, Thornberry NA, et al. Identification and inhibition of the ICE/CED-3 protease necessary for mammalian apoptosis. Nature 1995;376:37–43.
34. Schulte-Hermann R, Bursch W, Kraupp-Grasl B, Oberhammer F, Wagner A. Programmed cell death and its protective role with particular reference to apoptosis. Toxicol Lett 1992;64–65:569–574.
35. Oberhammer F, Bursch W, Tiefenbacher R, et al. Apoptosis is induced by transforming growth factor-beta 1 within 5 hours in regressing liver without significant fragmentation of the DNA. Hepatology 1993;8:1238–1246.
36. George J, Roulot D, Koteliansky VE, Bissell DM. In vivo inhibition of rat stellate cell activation by soluble transforming growth factor beta type II receptor: A potential new therapy for hepatic fibrosis. Proc Natl Acad Sci USA 1999; 96:12719–12724.

Develop. Growth Differ. (2008) **50**, 307–320 doi: 10.1111/j.1440-169x.2008.01034.x

Original Article

Identification and characterization of nucleoplasmin 3 as a histone-binding protein in embryonic stem cells

Natsuki Motoi,[1,2] Ken-ichi Suzuki,[1,2] Ryuichi Hirota,[3†] Penny Johnson,[4] Ken Oofusa,[3‡] Yutaka Kikuchi,[1] and Katsutoshi Yoshizato[1,2*§]

[1]*Developmental Biology Laboratory and* [2]*Hiroshima University 21st Century COE Program for Advanced Radiation Casualty Medicine, Department of Biological Science, Graduate School of Science, Hiroshima University, 1-3-1 Kagamiyama, Higashihiroshima, Hiroshima 739-8526,* [3]*ProPhoenix Company, 3-13-26, Kagamiyama, Higashihiroshima, Hiroshima 739-0046, Japan; and* [4]*Intercytex Company, Grafton Street, Manchester, M13 9XX, UK*

Embryonic stem (ES) cells are thought to have unique chromatin structures responsible for their capacity for self-renewal and pluripotency. To examine this possibility, we sought nuclear proteins in mouse ES cells that specifically bind to histones using a pull-down assay with synthetic peptides of histone H3 and H4 tail domain as baits. Nuclear proteins preferentially bound to the latter. We identified 45 proteins associated with the histone H4 tail and grouped them into four categories: 10 chromatin remodeling proteins, five histone chaperones, two histone modification-related proteins, and 28 other proteins. mRNA expression levels of 20 proteins selected from these 45 proteins were compared between undifferentiated and retinoic acid (RA)-induced differentiated ES cells. All of the genes were similarly expressed in both states of ES cells, except nucleoplasmin 3 (NPM3) that was expressed at a higher level in the undifferentiated cells. NPM3 proteins were localized in the nucleoli and nuclei of the cells and expression was decreased during RA-induced differentiation. When transfected with NPM3 gene, ES cells significantly increased their proliferation compared with control cells. The present study strongly suggests that NPM3 is a chromatin remodeling protein responsible for the unique chromatin structure and replicative capacity of ES cells.

Key words: chromatin remodeling, histone chaperone, histone modification, histone tail, retinoic acid.

Introduction

Embryonic stem (ES) cells are derived from the inner cell mass in mammalian blastocysts and possess two unique characteristics: self-renewal, the activity of unlimited cell propagation, and pluripotency, the capability to differentiate into multilineage cell types through various differentiation processes (Evans & Kaufman 1981).

Mouse ES cells require leukemia inhibitory factor (LIF) (Williams *et al.* 1988) in order to exhibit these unique characteristics. Researchers have reported several transcription factors that are involved in the uniqueness of ES cells: Oct4 and Nanog (Nichols *et al.* 1998; Chambers *et al.* 2003; Mitsui *et al.* 2003), and Stat3 and Sox2 (Matsuda *et al.* 1999; Masui *et al.* 2007). Recent studies have demonstrated that the forced coexpression of Oct3/4, Sox2, Klf4, and c-Myc induces reprogramming of mouse (Takahashi & Yamanaka 2006) and human somatic cells into pluripotent stem cells (iPS cells) (Takahashi *et al.* 2007).

Generally, the gene expression profile of a cell is considered to depend on its chromatin structure (Misteli 2001). The core unit of chromatin is the nucleosome, which is composed of a histone octamer

*Author to whom all correspondence should be addressed.
Email: katsutoshi.yoshizato@phoenixbio.co.jp
†Present address: Laboratory of Cell Engineering, Department of Molecular Biotechnology, Graduate School of Advanced Sciences of Matter, Hiroshima University, 1-3-1 Kagamiyama, Higashihiroshima, Hiroshima, 739-8526, Japan
‡Present address: Towa Environment Science Co., Ltd, ProPhoenix Division, 3-13-60, Kagamiyama, Higashihiroshima, Hiroshima 739-0046, Japan
§Present address: PhoenixBio Co., Ltd. 3-4-1, Kagamiyama, Higashihiroshima, 739-0046, Japan
Received 28 December 2007; revised 20 February 2008; accepted 27 February 2008.

consisting of two units each of four core histones, H2A, H2B, H3, and H4, and a 146-bp-long DNA sequence that wraps the histone octamer. Adjacent nucleosomes are connected together by linker DNA and histone H1. Recently, it has been reported that the major chromatin proteins such as core and linker histones, and heterochromatin protein 1 are uniquely associated in mouse ES cells, and that this is related to the highly plastic nature of their chromatin structures (Meshorer & Misteli 2006; Meshorer *et al.* 2006). Researchers have attempted to identify and characterize nuclear proteins specific to ES cells with large-scale proteomic analyses (Kurisaki *et al.* 2005; Nagano *et al.* 2005); however, the fine chromatin structures of ES cells remain largely unknown. The N-terminal tail domain of histone, also called the histone tail, protrudes from the surface of the nucleosome and is an important element in the functional state of chromatin. It is known that the histone tail interacts with the chromatin remodeling complex, which regulates transcriptional activity. Histone tails are biochemically modified through acetylation, methylation, phosphorylation, and ubiquitination which is essential for global transcriptional regulation (Turner 2002) and considered to be associated with epigenetic cell memory (Jenuwein & Allis 2001; Turner 2002).

In this study, we aimed to identify the nuclear proteins unique to ES cells. Nuclear proteins were prepared from mouse ES cells and subjected to affinity selection using histone tail peptides as baits. The tail peptide-associated proteins were identified and categorized into (I) chromatin remodeling proteins; (II) histone chaperones; (III) histone modification-related proteins; and (IV) others. Among them, we found that nucleoplasmin 3 (NPM3), a protein that belongs to the second category, is unique in that the protein was expressed at a higher level in undifferentiated ES cells compared with the ES cells that had been induced to differentiate toward neurons by retinoic acid (RA). NPM3 is a member of the nucleophosmin/nucleoplasmin (NPM) family (NPM1-3) that is ubiquitously present throughout the animal kingdom (Eirín-López *et al.* 2006; Frehlick *et al.* 2007). This family has important roles in cellular processes such as chromatin remodeling (Tamada *et al.* 2006), DNA duplication (Okuda 2002), and transcriptional regulation (Liu *et al.* 2007a). Importantly to our study, NPM 1 was reported to be involved in the proliferation of mouse ES cells and hematopoietic stem cells (Li *et al.* 2006; Wang *et al.* 2006). Thus, we characterized NPM3 further as to its role in the proliferation of ES cells. Our study indicates that NPM3 may play an important role in maintaining the unique chromatin structures of ES cells.

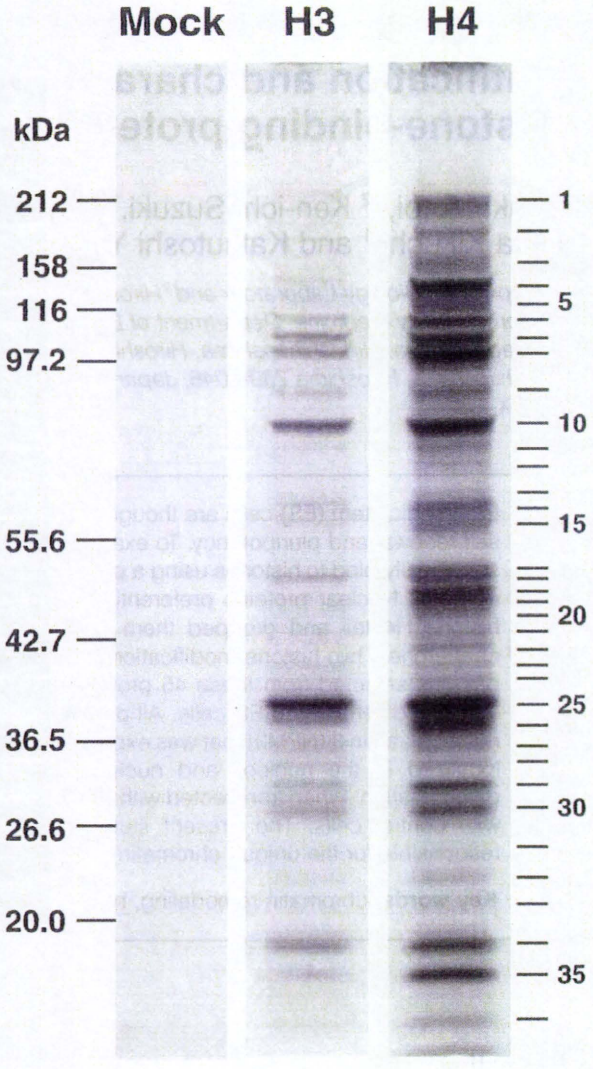

Fig. 1. Separation of histone tail-associated proteins by sodium dodecyl sulfate–polyacrylamide gel electrophoresis (SDS–PAGE). Nuclear extracts of CMT-1-ES cells were incubated with the beads bearing the H3 or H4 tail peptides. The binding experiments were carried out under the same conditions for both tail peptides. The bead-bound proteins were separated on 4–12% gradient SDS–PAGE and were stained with CBB R-250. The positions of molecular mass marker in kDa are indicated at the left side of the panel. The bands with Arabic numerals from 1 (top) to 36 (bottom) were cut off and subjected to protein identification by mass spectrometry. Identical banding patterns were observed in three independent analyses. 'Mock' represents a result using beads without histone tail peptides. There were no protein bands detected in the mock experiment, proving the specificity of protein binding to the beads.

Materials and methods

ES cell culture

Two types of mouse ES cell lines were used in this study: CMT-1-ES cells, which display a normal karyotype